Order Number 9130395

Complex formation between iodine and the triphenyl compounds of the group VA elements

Zhang, Yingru, Ph.D.

City University of New York, 1991

U·M·I
300 N. Zeeb Rd.
Ann Arbor, MI 48106

A

Complex Formation Between Iodine and the Triphenyl Compounds of the Group VA Elements

by

YINGRU ZHANG

A dissertation submitted to the Graduate Faculty
in Chemistry in partial fulfillment of the requirements
for the degree of Doctor of Philosophy,
The City University of New York

1991

This manuscript has been read and accepted for the Graduate Faculty in Chemistry in satisfaction of the dissertation requirement for the degree of Doctor of Philosophy.

4/26/91 — Date

Seymour Ruonson — Chair of Examining Committee

4/26/91 — Date

Richard Pike — Executive Officer

Richard Pike

Henry Ford

Supervisory Committee

The City University of New York

ABSTRACT

Complex Formation Between Iodine and the Triphenyl Compounds of the Group VA Elements

by

YINGRU ZHANG

ADVISOR: PROFESSOR SEYMOUR ARONSON

The iodine complexes of triphenylamine, triphenylphosphine, triphenylarsine and triphenylstibine were studied in the solid state and in organic solution.

In the solid state, the iodine complexes are stable over wide ranges of iodine concentration and are prepared by mixing the powder components. Triphenylstibine forms a liquid complex. By means of a solid state electrochemical technique, we have determined the Gibbs free energy of complex formation. The EMF data were obtained using solid electrochemical cells with an AgI electrolyte of the type:

$$\underset{(-)}{\text{Pt} \mid \text{Ag} \mid \text{AgI} \mid} \; \underset{(+)}{\text{I}_2\text{(c)} \mid \text{Pt}}$$

where $I_2(c)$ represents either pure or complexed iodine. The results indicate that the bond strengths between iodine and triphenyl compounds are in the order of P > As > Sb > N.

The electrical conductivities were also measured using the Van der Pauw four-probe technique for solid complexes and a two-probe method for

liquid complexes. Activation energies were calculated from the temperature dependence of the conductivity of the complexes.

Electrochemical experiments were performed which demonstrate that conduction in these complexes is primarily electronic.

In organic solution, an electrochemical technique was employed to study the ionization of the iodine complexes of Ph_3N, Ph_3P, Ph_3As, Ph_3Sb and pyridine.

EMF measurements were made in 1, 2-dichloroethane on concentration cells of the type:

$$Pt \mid I_2, R, TEAI(c) \text{ in } 1,2\text{-DCE} \parallel I_2, R \text{ in } 1, 2\text{-DCE} \mid Pt$$

where TEAI represents tetraethylammonium iodide, R is a symbol for organic compounds. In conjunction with electrical conductivity measurements and UV-VIS spectrophotometric analysis, several different ionization mechanisms were proposed depending on the chemical nature and concentration ratio of the reactants. Equilibrium constants were calculated from the EMF data for the various ionization steps.

A ^{31}P-NMR study was also performed to investigate the triphenylphosphine-iodine charge-transfer complex formation and ionization reactions.

ACKNOWLEDGEMENT

To Professor Seymour Aronson, I will be forever grateful. His excellent scientific guidance was expected, his understanding, friendship and caring went well beyond the call of duty. I could not have had a better beginning in the U.S.A. than starting and completing my graduate study with one of the best teachers I have ever had. I am proud to have worked under such a fine research scientist, his guidance and infinite patience have made this project possible.

I would like to give my special thanks to Professor Vojtech Fried who introduced me to, and assisted in my acceptance at Brooklyn College.

I wish to express my sincere thanks to Professors Richard Pizer and Henry Teoh, the members of my committee, for contributing their time and advice. Professor Gary Mennitt deserves my deep thanks for contributing his extensive knowledge of NMR spectroscopy.

It is a great pleasure to acknowledge Mr. Ottmar Safferling, my glassblowing teacher and good friend. The great help he provided with his utmost skill in glassblowing as well as the knowledge in wordprocessing with Macintosh was essential for this thesis work.

Finally, my further thanks and good wishes to Professors Dominick Labianca, Richard Pizer and Gary Mennitt who made my graduate years more rewarding and pleasurable with their friendship and thoughts.

CONTENTS

List of Tables

List of Figures

Chapter 1 INTRODUCTION

§.1-1 General Aspects

Since the 1960's, research interest in molecular complexes has been on the upsurge. Charge-transfer complexes are of interest not only because of the many intriguing possibilities of novel materials and their promising properties but also because a good theoretical understanding of the thermodynamic and electrical transport properties is still lacking.[1]

The iodine complexes of triphenylamine, triphenylphosphine, triphenylarsine and triphenylstibine are especially interesting because they give a useful set of n-donor, σ-acceptor systems where the donor strengths vary markedly. When the triphenyl compounds are complexed with iodine, the resulting system has semiconducting properities. When iodine reacts with the triphenyl compound in an organic solvent, the first step is the formation of an "outer complex" in which a small amount of charge transfer occurs. Then, the charge transfer may proceed further with the formation of an "inner complex" which is an ion-pair. The second step may be favored by a polar medium, a so-called solvent-assisted charge transfer reaction.

§.1-2 History

Modern interest in molecular complexes was awakened after the publication of the spectrophotometric studies of H. A. Benesi and J. H. Hildebrand on iodine complexes of aromatic substances in 1950. The extensive developments in this field are reflected by a steadily increasing number of papers and novel materials.

The iodine charge transfer complexes of the triphenyl group VA compounds were first studied in organic solution by Bhat[2] and Rao in 1966. The

transformation of the outer iodine complexes of triphenylarsine and triphenylstibine to their inner complexes has been reported to be a first order reaction. Bhat et al have shown that the rate constants are quite large and the transformation for $(Ph)_3AsI_2$ is faster than for $(Ph)_3SbI_2$.

Rao[3] and co-workers have made a study of the electronic spectra of iodine complexes of triphenyl group VA compounds in non-polar organic solution. They estimated that the ease of formation of the inner complex is in the order : $P(Ph)_3 > As(Ph)_3 > Sb(Ph)_3 > N(Ph)_3$.

In 1979, Sahai[4] and co-workers measured equilibrium constants of outer-complex formation in CCl_4 for these systems using electrical conductance and refractometric techniques. Their conductrometric titrations indicated 1:1 stoichiometry for these complexes. The conductance measurements of Sahai in dioxane and tetrahydrofuran and Beveridge[5] and coworkers in acetonitrile demonstrated that significant ionization of the complexes occurs.

A quantitative study of the ionization reaction by Aronson[6] on pyridine-iodine complexes indicates that, at high concentration ratios of pyridine to iodine, twenty-five per cent of the complex ionized in 1,2-dichloroethane.

In the solid state, the charge transfer complexes of iodine with the triphenyl compounds of N, P, As and Sb are still far from fully explored[7].

The reference by Steinkopf and Schwen in 1921 for the first time contains a passing mention of $(Ph)_3As\text{-}I_2$, which was not characterized. In 1964, Harris[8] and Beveridge noted the existence of $(Ph)_3As\text{-}I_4$ but still no characterization was reported.

Harris[8] and co-workers prepared the compounds $(Ph)_3P\text{-}I_2$, $(Ph)_3P\text{-}I_4$, $(Ph)_3As\text{-}I_2$, $(Ph)_3As\text{-}I_4$ and $(Ph)_3Sb\text{-}I_2$ by crystallization from CH_3CN. Their conductances in CH_3CN solution were also reported.

In 1980, Harris and Farhat reported conductance studies of many "halogen adducts" of $(Ph)_3P$, but mostly with mixed sets of halogens.

Cotton[9] and Kibala recently determined the crystal structures of $(Ph)_3P\text{-}I_4$ and $(Ph)_3As\text{-}I_4$. Their x-ray analysis indicated that the structures crystallized from dichloroethane solutions were $[(Ph_3PI)_2I_3]^+I_3^-$ and $[(Ph_3AsI)_2I_3]^+I_3^-$. The structure of the phosphorus complex crystallized from toluene solution was $(Ph_3PI^+)I_3^-$.

Several studies have recently been made to determine free energies of formation of iodine-organic complexes using AgI as a solid electrolyte in electrochemical cells. These studies include the iodine complexes of metallophtalocyanines[10], phenothiazine[11], phenazine[12] and polyacrylonitrile[13].

Chapter 2 THEORETICAL

§.2-1 Charge-Transfer Theory

In 1950, Mulliken[14] provided a satisfactory explanation of the characteristic electronic absorption in terms of an intermolecular charge-transfer transition — the Charge Transfer Model. Following Mulliken's quantum mechanical treatment of charge transfer complexes between a donor(D) and an acceptor(A), the ground-state wave function for the donor-acceptor complex (D. A) has the form:

$$\Psi_N (D{\cdot}A) = a\psi_0(D,A) + b\psi_1(D^+\text{-}A^-) + \cdots \qquad (2.1\text{-}1)$$

where $\psi_0(D,A)$ denotes a "no-bond" structure, in which the two molecular species interact with ordinary intermolecular forces and $\psi_1(D^+\text{-}A^-)$ is the "dative" wave function representing transfer of an electron from donor to acceptor. The "a" and "b" are normalization constants whose relative magnitudes define the extent of charge transfer.

Mulliken's charge transfer model implies that the complex is stabilized by the resonance between the "no-bond" structure Ψ_0 and the "dative" structure Ψ_1. The strength and stability of donor-acceptor interaction are dependent on the extent of charge transfer. When $b > a$, Ψ_1 prevails and complexation is stronger. When $b << a$ in the case of loose complexes (outer complexes), a very small but non-zero contribution of the charge-transfer structure stabilizes the complex.

According to quantum-theory principles, there must be an excited-

state Ψ_E, corresponding to the ground-state Ψ_N, where

$$\Psi_E\,(D{\cdot}A) = -b^*\psi_0(D,A) + a^*\psi_1(D^+\text{-}A^-) + \cdots \qquad (2.1\text{-}2)$$

Therefore, the spectrum of a molecular complex then consists of a unique absorption due to the transition from the ground to excited state of the complex — a so-called "charge-transfer band".

§.2-2 Common Types and Strength of Donors and Acceptors

Mulliken has divided even-electron donor and acceptor species into increvalent and sacrificial types[14]. The common types of donors and acceptors are listed in Table (2-I).

In increvalent donors, donation of one electron is from a lone pair located on the key atom (such as :N in R_3N), the nitrogen valence increases from 3 to 4. I_2 is a sacrificial σ acceptor, the acceptance of an electron into its σ_n molecular orbital leading to I_2^- weakens the bond between the atoms. As a result of a compromise geometry between I_2 and I_2^- (as in Ψ_0 and Ψ_1 term of Eq.(2.1-1), respectively), the I-I bond length in a complex is longer than that in ordinary I_2 and shorter than that in I_2^-.

Increvalent acceptors are vacant-orbit (ν) acceptors whose functioning in the Ψ_1 term of Eq.(2.1-1) is similar to that of increvalent donors. The behavior of sacrificial donors is similar to sacrificial acceptors.

In general, $n{\cdot}\nu$ charge-transfer leads to the strongest complex and $\pi{\cdot}\pi$ interaction gives the weakest complex. This conclusion is based on the general fact that a stronger donor or acceptor tends to make b/a larger in

Table (2-I):

The Common Types of Donors and Acceptors [13]

Donor

Structure Type	Function Type	Dative Electron From	Examples
n	Increvalent	Nonbonding lone pair	: NR_3
b	Sacrificial	Bonding orbtial	Benzene
b	Sacrificial	Bonding orbtial	RX

Acceptor

Structure Type	Function Type	Dative Electron From	Example
v	Increvalent	Vacant orbital	BCl_3
a	Sacrificial	Antibonding orbtial	TCNE*
a	Sacrificial	Antibonding orbtial	Iodine

*: TCNE stands for tetracyanoethylene.

Eq.(2.1-1), hence, complexation is stronger.

What factors determine the strength of donors and acceptors? In view of the Charge-Transfer Resonance Model, donor ability increases with decreasing ionization potential I and acceptor ability with decreasing electron affinity E. Nevertheless, Mulliken has pointed out that the geometric factors (such as mutual approachability) are often important. Therefore, a good donor should have small I and good approachability.

Another effect is equally important in considering the strength of the donor-acceptor interaction[15] — Two-way Donor-Acceptor Action (also called "backbonding" or "synergistic action").

Some donors, so-called amphodonors, such as P and S, have low-lying d-orbitals so they can function not only as n-donors but as ν-acceptors in a two-way action, whereas the others like N and O have empty d-orbitals only at higher energies and so they have no function except that as n-donors. Obviously, the back-bonding enhances the donor-acceptor interaction and the amphodonor or amphoacceptor is more efficient in the complexation than an one-way donor or acceptor.

§.2-3 Inner and Outer Complexes

Mulliken qualitatively described the energy of interaction between donors and acceptors as a function of a charge-transfer reaction coordinate, "c". Without a precise definition, c is used as a quantity which continuously increases with charge-transfer (that is, with increasing b/a in Eqs.(2.1-1)). Several plausible forms of the potential energy diagram[13] for the interactions between a donor and an acceptor with varying degrees of environ-

mental assistance are shown in Figure (2.1). There are two minima in curves I and II, one at small c corresponding to $b^2 \ll a^2$ is for the outer complex, another, which was taken as defining c=1, corresponding to $b^2 \cong a^2$ or $b^2 > a^2$, is for the inner complex. The maximum between these minima is an activated complex.

The inner complex is an ion-pair and the activated complex is the intermediate between the inner and outer complexes. Increasing c corresponds to increasing ionic character in the wave function. Therefore, a polar solvent must lower the energy more and more as c increases. Solvation will stabilize the inner complex to a greater extent than the outer complex. The activation energy should decrease with increasing solvent dielectric constant, (Figure (2.1) curve I and II). So under a sufficient influence of a polar solvent, the inner complex becomes the more stable form of the donor-acceptor pair (curve II). For many strong complexes (such as n·ν complexes), particularly in a solvent with high-dielectric constant, a single deep minimum corresponding to the inner complex with extensive charge transfer is typical, (curve III).

If the inner complex becomes the energetically more stable form, more or less complete dissociation into solvated ions may occur as a secondary process.

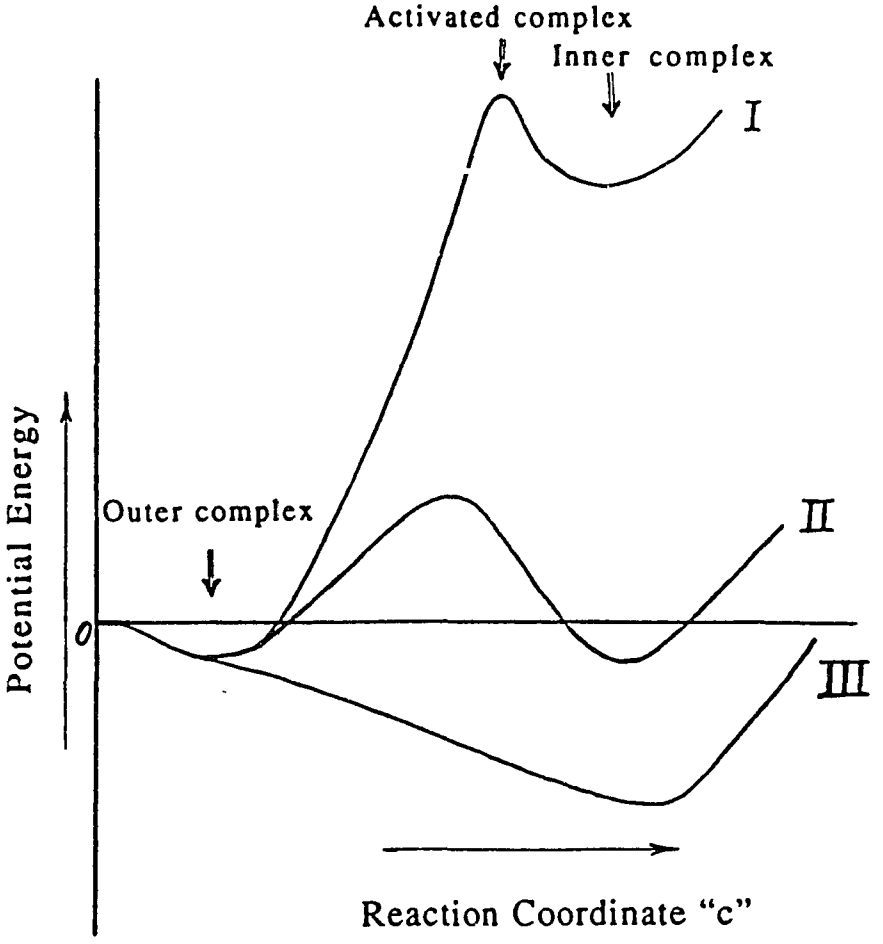

Figure (2.1) :

Potential energy diagram for interaction between a donor and acceptor with varying degrees of environmental assistance: **curve I**, unassisted; **curve II**, assisted by a rather low-dielectric solvent; **curve III**, assisted by a high-dielectric solvent.

§.2-4 NMR Spectra

Interaction of a nucleus with its electronic environment, especially the valence electrons, influences the magnetic resonance absorption of the nucleus.[16] At resonance, a change in the electronic environment within the atom so that the magnetic field at the nucleus is enhanced or reduced necessitates a change in the applied magnetic field. Such a change is called a chemical shift which is measured in parts per million (ppm) of the applied magnetic field relative to a chemical compound chosen as a reference. Since phosphorus has spin 1/2, a high magnetic moment, 100% natural abundance and its NMR has uncrowded chemical shifts,[17] ^{31}P NMR spectroscopy has become a powerful tool in the analysis of organic phosphorus compounds and coordinate complexes.

The magnetic resonance spectrum of a nucleus can exist in more than one chemical environment and its appearance is dependent on its lifetimes in these different environments[18]. Consider the case of two environments, I and II, in either of which alone it is a singlet. If the lifetimes in the two states are 10 to 1000 times longer than $\sqrt{2}\,(\pi\,|\,\delta_I-\delta_{II}\,|\,H)^{-1}$ (where δ_I and δ_{II} stand for the two chemical shifts if each absorption appeared singly and $|\,\delta_I-\delta_{II}\,|\,H$ is the frequency difference in Hz) then two lines are observed. If the lifetimes are 1 to 100 times shorter than $\sqrt{2}\,(\pi\,|\,\delta_I-\delta_{II}\,|\,H)^{-1}$, then there is only a single, time-average line whose position is dependent on the relative populations[19], P_I and P_{II} in the two environments:

$$\delta = P_I\delta_I + P_{II}\delta_{II} \qquad (2.4\text{-}1)$$

The observed chemical shift δ of the broadened-line is influenced by

changes in factors such as concentration and temperature which cause an alteration in P_I and P_{II}.

It is anticipated that we may observe such chemical shift changes resulting from some equilibria involved in complex-formation or complex-dissociation reactions of the charge transfer complexes.

§.2-5 Electrical Conduction Mechanisms For Organic Materials

Vast numbers of organic materials are generally considered to be electrical insulators. However, since the 1960's, an increasing number of organic compounds have been discovered to exhibit interesting and useful electrical characteristics. Although considerable experimental work has been carried out on the preparation and study of the electronic properties of these materials, no comprehensive theory for conduction has yet been proposed.

2.5-1 Band Theory and Hopping Model

The most widely used explanations of the experimentally observed conduction phenomena in organic charge-transfer complexes are in terms of an electronic band model and a hopping model.

Bloch solved the Schroedinger equation with a periodic potential arising from the lattice atoms. The solutions were of the form:

$$\Psi_K = e^{ikx}\mu_K(x) \qquad (2.5\text{-}1)$$

where k is the wave number and $\mu_k(x)$ is a periodic function whose period is the lattice constant, a. The energy dependence of free electrons on wave number is given by the following equation:

$$E_K = \frac{h^2}{2m} k^2 \qquad (2.5\text{-}2)$$

The energy dependence for electrons in a periodic lattice described by Eqs. (2.5-1) and (2.5-2) is shown in Figure (2.2)[20]. Thus there are allowed and forbidden ranges of energy. They correspond to the energy band calculated by overlap integrals of molecular wave functions between adjacent molecules. The relative weakness of the intermolecular interaction of charge-transfer complexes results in rather narrow conduction bands and low carrier mobilities.

The band model has been widely used to explain many experimental results. However, it is not applicable to all systems. Particularly for materials which exhibit a periodic lattice and very small carrier concentrations and mobilities, the band model may be replaced by a hopping model.

In organic crystals, the overlaps of the molecular orbital are generally very small. The orbital of one molecule, therefore, can be considered to be isolated from that of others. Thus, conduction involves an energy barrier for an electron to "hop" from one molecule to the next.

2.5-2 Conductivity of Organic Semiconductors

Conductivity, in general, is given by the equation:

$$\sigma = N \cdot q \cdot \mu \qquad (2.5\text{-}3)$$

N is the concentration of current carriers, q is the electric charge on a carrier, and μ is the mobility. The concentration of the current carriers should vary with temperature according to the following relationship:

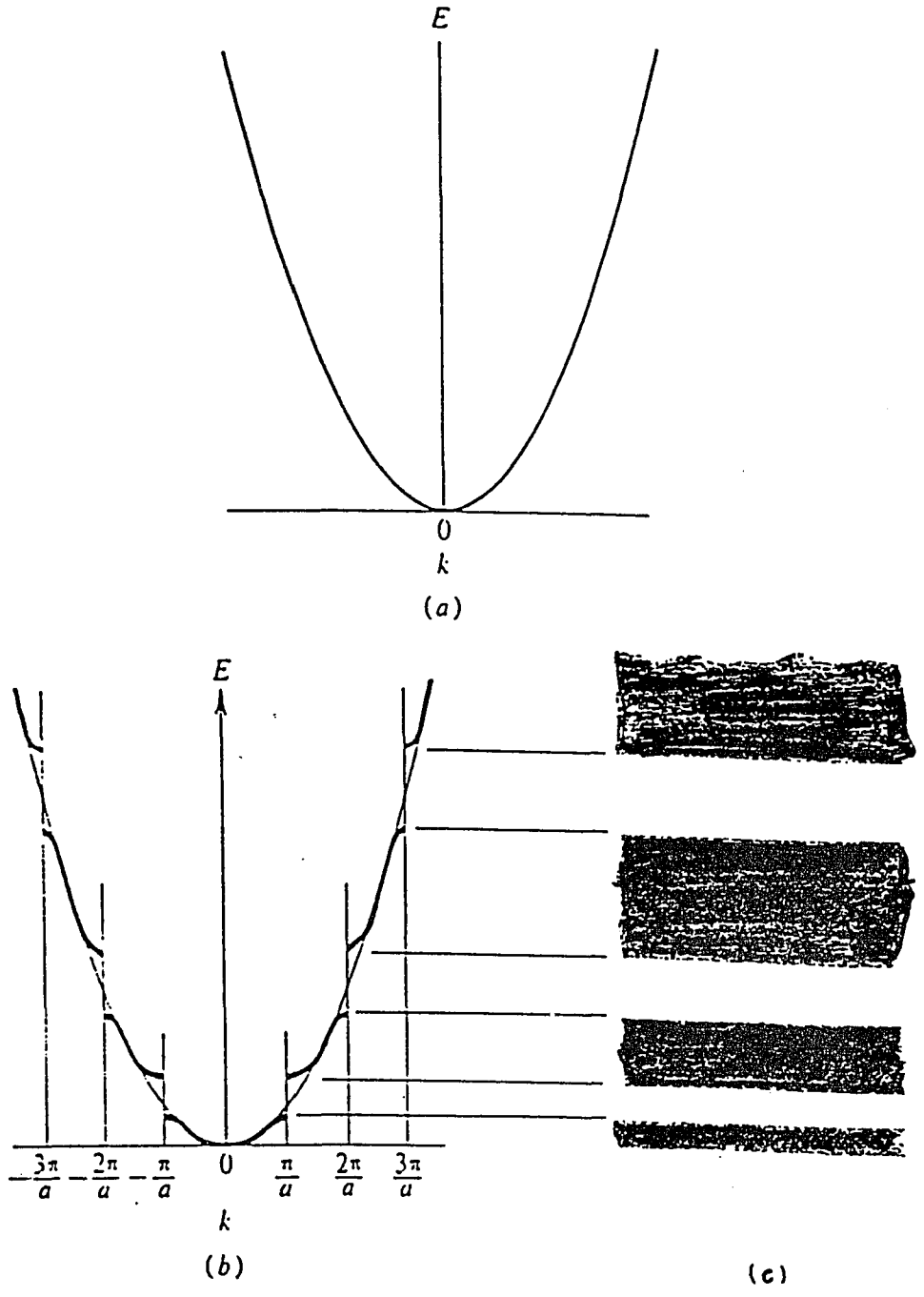

[20]

Figure (2.2):
Electron energies as a function of wave number, for (a) free electrons, and (b) electrons moving in a periodic potential. The allowed energy bands (as a function of distance through the crystal) are shown in (c).

$$N = N_0 \exp(-\varepsilon/2kT) \qquad (2.5\text{-}4)$$

where k is Boltzmann's constant, N_0 is a constant and ε is the energy gap between the valence and conduction band. It is assumed that the mobility varies slowly with temperature. From Eqs. (2.5-3) and (2.5-4), we can write the conductivity as follows:

$$\sigma = q \cdot \mu \cdot N_0 \cdot \exp(-E/kT) = \sigma_0 \cdot \exp(-E/kT) \qquad (2.5\text{-}5)$$

where σ_0 is a constant and E is the activition energy, which is equal to $\varepsilon/2$.

2.5-3 Liquid Conductors

There are three liquid types which were classified according to their electrical conductivity by Mott[21] shown in Table (2-II). Their conductivities can be calculated by different equations. For metallic liquids, conductivity is determined by calculating the Fermi wave number k_F according to free electron theory and evaluating the electronic mean free path, ^, using x-ray diffraction techniques. For semi-metallic liquids, Mott argued that the density of states at the Fermi energy $n(E_F)$ rather than ^ becomes the controlling factor, Eq. (2.5-7). For insulating and semi-conducting liquids which corresponds to $\sigma < 300\ (\Omega cm)^{-1}$, the conductivity arises from the thermal excitation of carriers across the mobility gap or by hopping processes. The semi-empirical equation Eq.(2.5-5) is used to calculate the conductivity.

Table (2-II)[21]

Conductivities of Liquid Semiconductors

Liquid Type	Magnitude of Conductivity	Conductivity Expression
Metallic liquids (eg. mercury)	>3,000 $\Omega^{-1}cm^{-1}$	$\sigma = \frac{k_F^2 e^2 \wedge}{3\pi^2 h}$ (2.5-6) k_F: Fermi wave number $\wedge$: ele. mean free path
Semi-metallic Liquids (eg. Sb_2S_3, Cu_2S in liquid state)	300 to 3,000 $(\Omega cm)^{-1}$	$\sigma = \frac{g^2 e^2}{3hd}$ (2.5-7) $g = n(E_F)/n_0(E_F)$ $n_0(E_F)$: free ele. density d: interatomic spacing
Insulating and Semiconducting Liquids (eg. CuI in liquid state)	< 300 $\Omega^{-1}cm^{-1}$	$\sigma = \sigma_0 \cdot \exp(-E/kT)$ (2.5-5) σ_0 is a constance.

2.5-4 The Thermodynamic Function For the Relative Integral Molar Free Energy

Lewis and Randall have defined a "relative" partial quantity as the difference between a partial molar quantity of a component in solution and the molar quantity of the pure substance in the reference state.

The *relative integral molar free energy* $\Delta_M G$ is defined as the difference between the sum of the free energies of the pure substances per mole, and the *free energy of one mole of the solution,* G_m. For example, in a binary solution:

$$\Delta_M G = \overline{G}_m^0 - (x_1 G_1^0 + x_2 G_2^0) \qquad (2.6\text{-}1)$$

$$\overline{G}_m^0 = (x_1 \overline{G_1} + x_2 \overline{G_2}) \qquad (2.6\text{-}2)$$

$$\Delta_M G = x_1(\overline{G_1} - G_1^0) + x_2(\overline{G_2} - G_2^0) \qquad (2.6\text{-}3)$$

where $\overline{G}_1$ and $\overline{G}_2$ are the *partial molar free energy* of species 1 and 2 in solution, respectively.

G_1^0 and G_2^0 are the *molar free energy of pure substances* 1 and 2 , respectively.

x_1 and x_2 are the *mole fractions* of substances of 1 and 2 respectively in the binary solution.

$(\overline{G_1} - G_1^0)$ and $(\overline{G_2} - G_2^0)$ are the changes in free energy resulting from mixing one mole of pure substances 1 and 2 with an infinite quantity of solution. $(\overline{G_i} - G_i^0)$ is , by definition , the *relative partial molar free energy of substance i.* Thus,

$$\Delta_M\bar{G}_1 = \bar{G}_1 - G_1^0$$

$$\Delta_M\bar{G}_2 = \bar{G}_2 - G_2^0 \qquad (2.6\text{-}4)$$

Substituting Eq. (2.6-4) into Eq. (2.6-3), we obtain

$$\Delta_M\bar{G} = x_1\Delta_M G_1 + x_2\Delta_M G_2 \qquad (2.6\text{-}5)$$

from the Gibbs-Duhen relation, it follows that

$$x_1\left(\frac{\partial\Delta_M G_1}{\partial x_2}\right) + x_2\left(\frac{\partial\Delta_M G_2}{\partial x_2}\right) = 0 \qquad (2.6\text{-}6)$$

We can rewrite the equation in the form:

$$\Delta_M G_1(x_2) = -\int_0^{x_2} \frac{x_2}{1-x_2}\frac{\partial\Delta_M G_2}{\partial x_2}\,dx_2 \qquad (2.6\text{-}7)$$

The lower limit of integration in the equation is for pure substance 1, ie. $x_2 = 0, \Delta_M G_1 = 0$.

Integrating Eq. (2.6-7) by parts, we obtain the following equation:

$$\Delta_M G_1(x_2) = \int_0^{x_2} \frac{\Delta_M G_2}{(1-x_2)^2}\,dx_2 - \frac{x_2.\Delta_M G_2}{(1-x_2)} \qquad (2.6\text{-}8)$$

Substituting Eq. (2.6-8) into Eq.(2.6-5), we obtain

$$\Delta_M G = x_1\left[\int_0^{x_2} \frac{\Delta_M G_2}{(1-x_2)^2}\,dx_2 - \frac{x_2.\Delta_M G_2}{(1-x_2)}\right] + x_2\cdot\Delta_M G_2 \qquad (2.6\text{-}9)$$

Thus, the free energy change for the reversible and isothermal formation of one mole of solution or complex from x_1 moles of pure substance 1 and x_2 moles of pure substance 2 can be calculated by the following equation:

$$\Delta_M G = (1- x_2)\int_0^{x_2} \frac{\Delta_M G_2}{(1-x_2)^2} dx_2 \qquad (2.6\text{-}10)$$

Chapter 3 EXPERIMENTAL

§.3-1 CHEMICALS

Triphenylamine, -phosphine, -arsine, -stibine, 2,4,6-tri(2-pyridyl)-1,3,5-triazine, iodine, silver(60-mesh) and silver iodide (99.9%) were purchased in the highest commercial grades available from Aldrich Chemical Co. of Milwaukee, Wisconsin.

Reagent grade iodine was resublimed at 150°C under vacuum and kept in a tightly closed container. Silver iodide was recycled from 160°C to room temperature several times. Graphite powder (No.635) was obtained from Joseph Dixon Co. of Jersey City, N.J. Tetraethylammonium iodide was obtained in high purity from Alfa Chemicals Co.

§.3-2 IODINE ABSORPTION MEASUREMENTS

Experiments were conducted to determine the extent to which iodine is absorbed by the organic compounds. The maximum uptake of iodine by each of the triphenyl compounds at room temperature was determined by using the apparatus depicted in Figure (3.1). A weighed sample of triphenyl compound was placed in a vial above an excess amount of solid iodine in an evacuated tube. Contact between the substances was only through the gas phase. The amount of iodine absorbed by the triphenyl compound was determined by measuring the weight change from day to day until no further change occurred. The time to reach maximum uptake ranged from less than four days in the case of triphenylphosphine to twenty-five days in the case

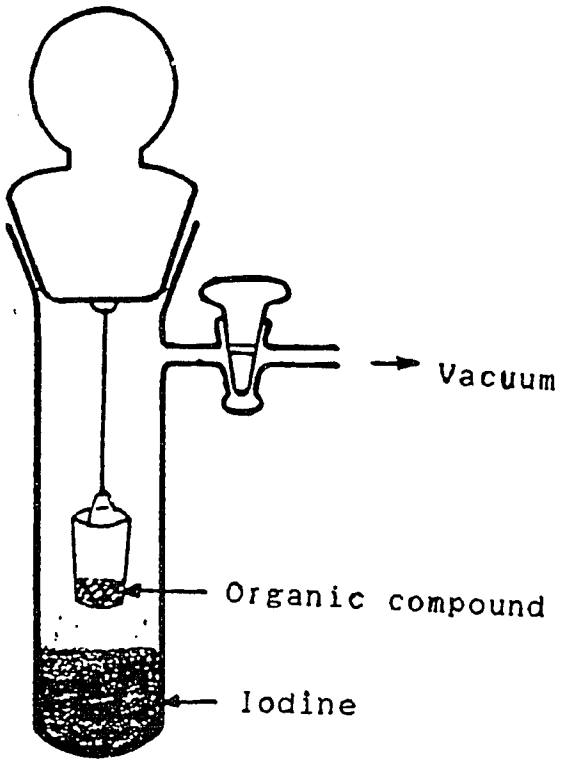

Figrue (3.1): Apparatus for vapor absorption measurements

of triphenylstibine.

Designated compositions of iodine-triphenyl compound were prepared by thoroughly mixing and grinding appropriate amounts of the two solid substances, sealing in evacuated glass tubes, and holding at room temperature for 48 hours.

Since triphenylantimony reacts with iodine forming a liquid complex, to prepare a homogeneous binary phase of liquid mixture, it is easier to use the apparatus in Figure (3.1). Specific mole ratios of iodine to triphenylantimony were obtained by the absorption of iodine by triphenylantimony during a predetermined time period. The mixtures were then placed in empty evacuated tubes for another day and reweighed.

§.3-3 CONDUCTIVITY MEASUREMENTS

3.3-1 Complexes Formed By Mixing Solid Components

Electrical conductivity measurements on the solid iodine complexes were made by the four probe Van der Pauw technique.[22,23] The powder samples were compacted at a pressure of 25 ton/inch^2, using a 30 ton pellet press Model M-30. The solid cylindrical pellets were fabricated in the form of discs of uniform thickness, about 0.15 cm, and 1.3 cm in diameter. In the apparatus shown in Figure (3.2), the pellet was placed under the four thin platinum-coated copper probes which were drilled through one piece of plastic. The four holes on the plastic fixed the probes, symmetrically contacting with the pellet at the periphery. Currents ranging from 0.1 to 50 microampers were passed through points (a) and (b) using a power supply Model 5005T from Power Designs Inc., Westbury, New York. The currents (I) were read with a Keithley Model 169 digital multimeter in the circuit. The corresponding voltages (V) were measured between (c) and (d) with another Keithley multime-

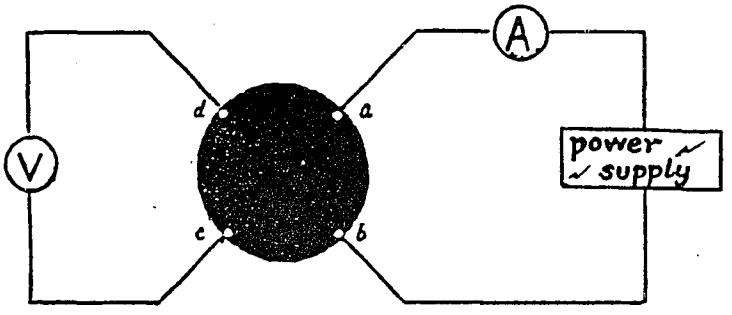

Figure (3.2) :

Apparatus for conductivity measurements of solid complexes

ter.

The conductivity was then calculated by the following equation:

$$\sigma = \left[\frac{\ln 2}{t \cdot \pi}\right] \cdot \left[\frac{1}{V}\right] \qquad (3.3\text{-}1)$$

where t is the pellet thickness.

A two-probe method[24] was used in measuring the conductivities of liquid compositions of $(Ph)_3Sb(I_2)_x$. As shown in Figure (3.3), a U-shape cell was used, consisting of two 10 mm i.d. vertical sections connected by a 25 cm long capillary tube. Electrical leads were clipped to graphite rods serving as electrodes.

The U-tube conductivity cells were calibrated with the graphite rods in position using 0.100 M and 1.00 M solutions of potassium chloride in distilled water at room temperature. The cell constant was calculated using the resistance of the potassium chloride solutions measured with an ac conductivity bridge.

The ac and dc measurements of resistance of triphenylantimony-iodine complex were made using a YSI Model 31 conductivity bridge and a Keithley Model 169 multimeter.

3.3-2 Complexes Formed In Organic Solution

Conductivity measurements on iodine complexes in 1,2-dichloroethane were made using a YSI-3402 Standard Dip Conductivity cell and a YSI Model 31 conductivity bridge.

The cells were cleaned by immersion in concentrated nitric acid and cleaning solution and then were repeatedly rinsed with distilled water and left standing in water until reuse. All solutions were pro-

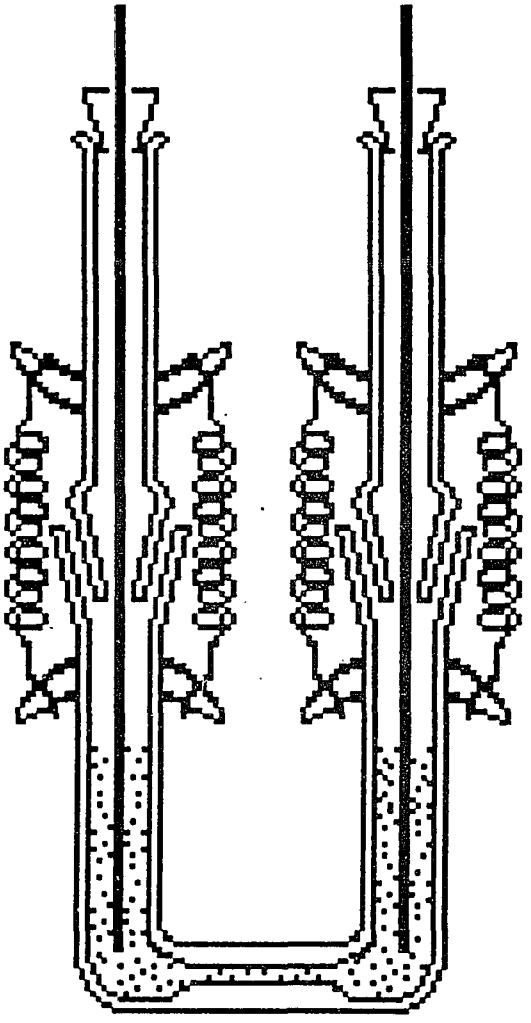

Figure 3.3: Two-probe Cell for Conductivity Measurements

tected from light by storing in the dark between periods of measurement.

§. 3-4 ELECTROMOTIVE FORCE MEASUREMENTS

3.4-1 Solid Electrochemical Cells For the Solid and Liquid Complexes

The EMF measurements on complexes formed by mixing solid components were performed using electrochemical cells with an AgI electrolyte.

The cell for solid complexes was prepared by the following procedure. Iodinated triphenyl compound was first uniformly mixed with 10% to 20% graphite which served as an inert, electrically conducting medium in the cathode. The mixture, the silver iodide, and the silver powder were each, preliminarily, pressed into pellets with maximum pressure by hand in a cylinder of 13 mm in diameter, and then the electrolyte layer was placed between the complex mixture and the silver powder discs. Using a hydraulic pellet press with vacuum attachment, the three layers were compressed together into a pellet at a pressure of 20 ton/inch^2. The compact was placed in the cell shown in Figure (3.4). Pieces of platinum foil, attached to platinum wires, were used for electrical contacts.

Triphenylantimony-iodine complexes are liquid at room temperature. We used the apparatus shown in Figure (3.5) to measure the EMF. The following procedure was used to prepare this cell. A layer of silver iodide powder was pressed on top of a layer of pressed silver powder. The liquid mixture was poured on top of the silver-silver iodide pellet. A graphite rod was insert into the liquid through a hole in the cover. At the bottom, a piece of platinum foil, attached to a platinum lead, was pressed up to contact the silver surface using a metal spring. The voltage between the graphite rode and the platinum lead was read.

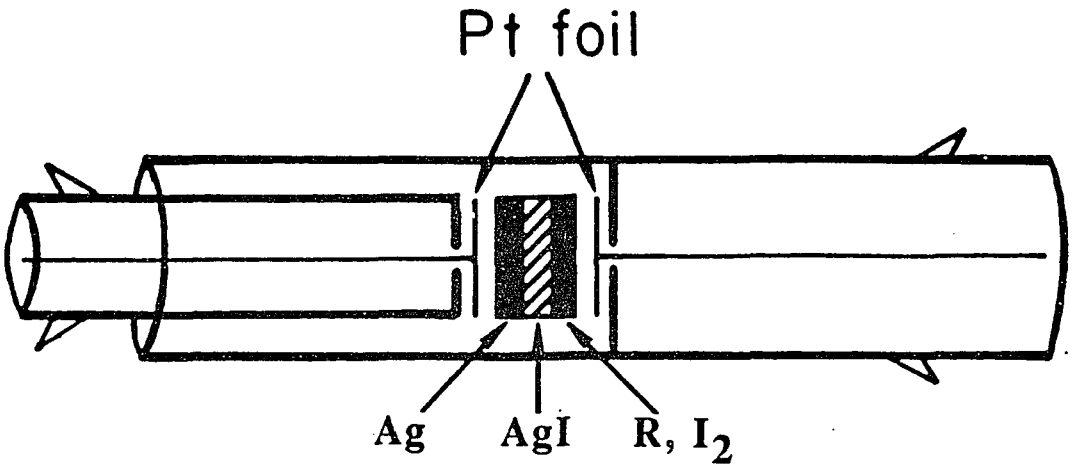

$$\overset{(-)}{\text{Pt} \mid \text{Ag} \mid \text{AgI} \mid \text{R}, \text{I}_2 \mid \text{Pt}} \overset{(+)}{}$$

Figure (3.4) : Cell for EMF measurements of solid complex

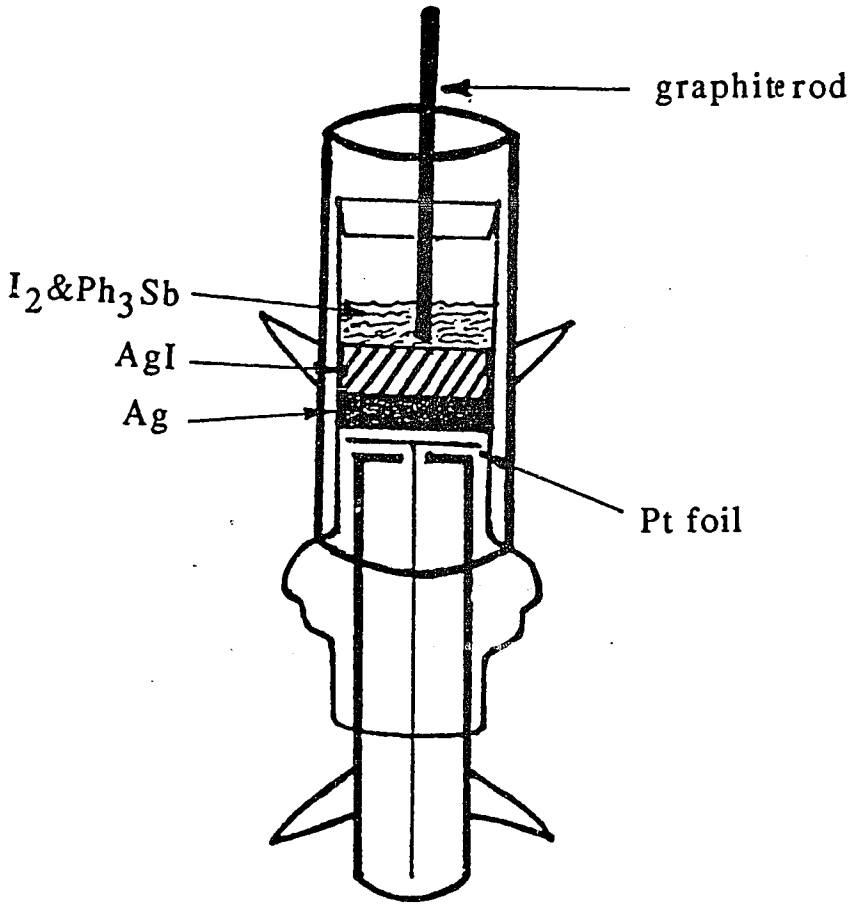

Figure (3.5) : Cell for EMF measurements of liquid complexes

EMF measurements were made at room temperature using a Keithley 169 electronic multimeter. In general, the EMF reading on a sample reached a steady value in about 20 minutes. The final EMF readings were not taken until the values had remained constant for a half hour. It was noted that for systems possessing two-phase regions, such as the triphenylantimony-iodine system, the equilibrium EMF values were much more rapidly reached and were more stable than those for the systems which formed a continuum of solid solutions. The EMF values were generally the same within ±10 mv for different batches of sample of the same composition.

3.4-2 Concentration Cells For Complexes In Organic Solution

EMF measurements for complexes in organic solution were made on concentration cells of the form:

$$Pt \mid I_2, R, TEAI(c) \text{ in DCE} \parallel I_2, R \text{ in DCE} \mid Pt$$

The cell design is shown in Figure (3.6). The H-shape cell consists of two compartments which are separated by a fine-frit disc. Both compartments were filled to the same level. Pieces of platinum foil attached to platinum wire leads were inserted into each compartment to [illegible]

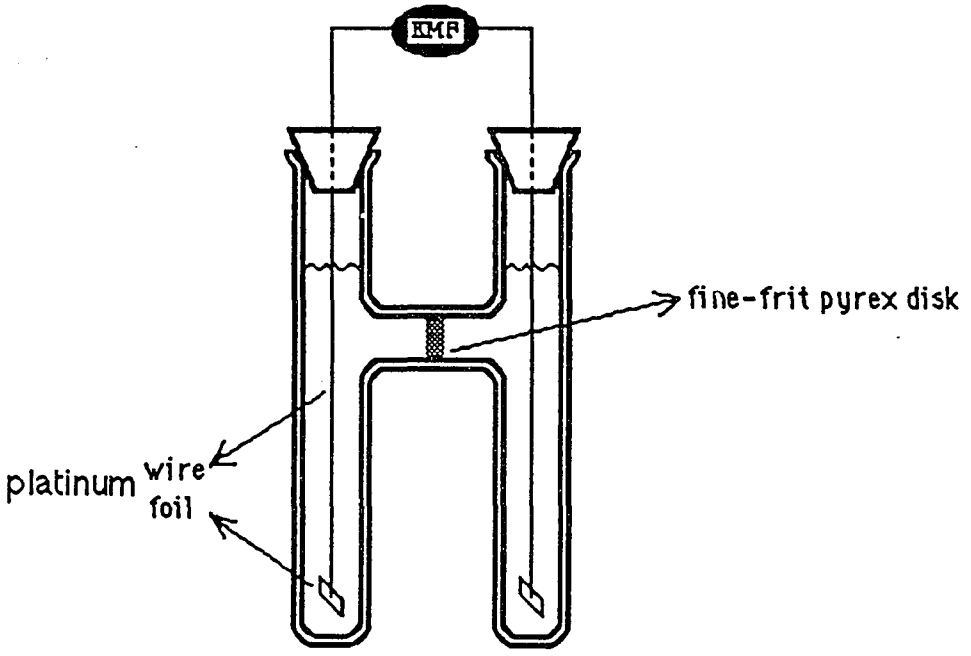

Figure (3.6): Concentration cell for EMF measurements

§. 3-5 UV-VIS SPECTRA MEASUREMENTS

Ultraviolet-visible absorption measurements on iodine complexes in 1.2-dichloroethane were made using a PERKIN-ELMER Lambda 3B UV-VIS spectrophotometer with PECSS UV-VIS Data Station and R-1000A Chart Recorder. Quartz cells of 10 mm and 2 mm thickness were used in these measurements.

§. 3-6 NMR SPECTRA MEASUREMENT

The measurements were made with the Bruker AC 250Mc high resolution Fourier transform nuclear magnetic resonance spectrometer that has ^{31}P monitoring capability with superconducting solenoids cooled by liquid helium.

Triphenylphosphine-iodine complexes in 1,2-dichloroethane were contained in 10 mm cylindrical quartz tubes. A locking signal was obtained by using an concentric tube containing D_2O inserted into the sample tube.

Eighty-five per cent orthophosphoric acid in a sealed 10 mm tube, obtained from Milwad Glass Co. Inc., Buena N.J., was used as an external reference standard. Precision by using an external standard is limited because of the difference in the bulk properties of the samples and the linearity of the field sweep. The use of an external standard was justified on the basis of a lesser need for precision when the chemical shift range is very large, as in our study of phosphorus NMR.

Chapter 4 THERMODYNAMIC AND ELECTRICAL PROPERTIES IN THE SOLID STATE

§.4-1 Compounds Used In the Study

Iodine reacts with a variety of organic compounds in the solid state to form charge-transfer complexes. Nine organic compounds have been studied whose structures are shown in Figure (4.1).

The most important compounds used in this study are the four triphenyl compounds of group VA: triphenylamine, triphenylphosphine, triphenylarsine and triphenylstibine. As an increvalent donor, the key atoms in the compounds (N, P, As and Sb) react with iodine to different extents to form n-donor, σ–acceptor charge-transfer complexes.

2,4,6-Tri(2-pyridyl)-1,3,5-triazine, 2,4,6-triphenyl-1,3,5-triazine and 1,3,5-Triphenyl benzene were also selected for the study. These compounds are similar to each other in that three phenyl or pyridyl groups are connected to a central benzene or aromatic nitrogen ring with single bonds, and they are different from one another in the number and location of the nitrogen atoms. These organic compounds may give us information about the contributions of the aromatic rings and the nitrogen atoms to the charge-transfer interaction with iodine.

A condensed aromatic nitrogen compound may exhibit larger charge density donation because of fewer steric effects compared with the compounds discussed above. Two condensed aromatic organic compounds, phenazine and acridine, were, therefore, also studied.

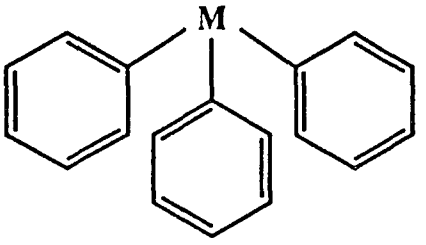

M = N, P, As or Sb

Triphenyl Group VA Compounds

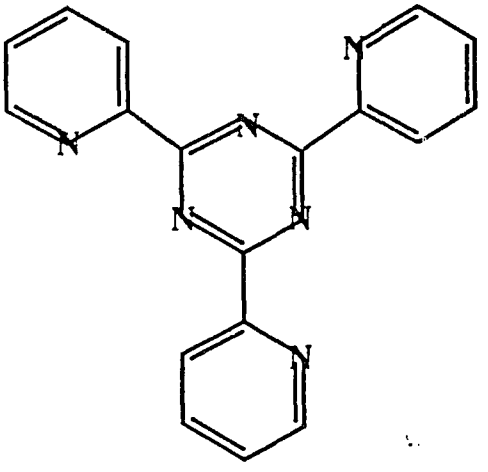

2,4,6-Tri(2-pyridyl)-1,3,5-triazine

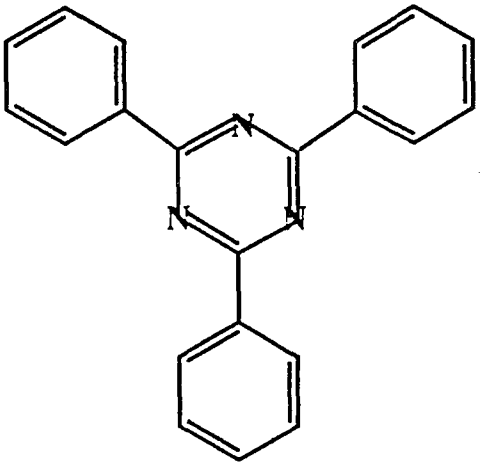

2,4,6,-Triphenyl-1,3,5-triazine

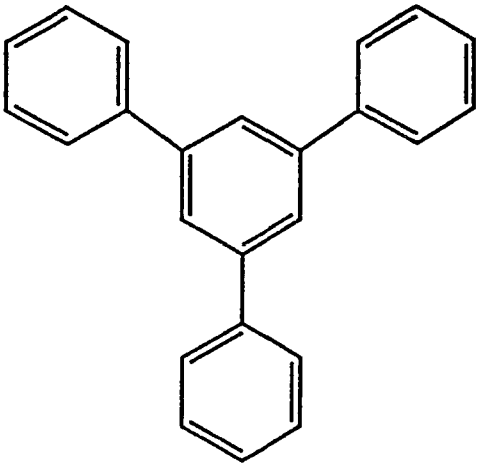

1,3,5-Triphenyl benzen

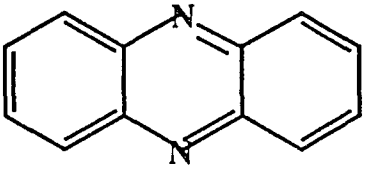

Phenazine

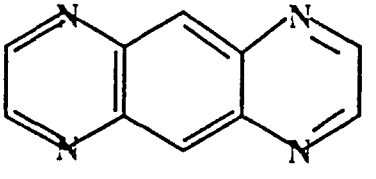

Acridine

Figure(4.1) Organic Compounds Used In the Study

§.4.2 Thermodynamic Stability

4.2-1 Electrochemical Behavior

EMF data were obtained on electrochemical cells of the type, I_2(c) | AgI | Ag at 25°C. I_2(c) represents pure iodine or iodine complexed in varying amounts with one of the organic compounds. The EMF data for the iodine complexes are plotted as a function of *the mole ratio of molecular iodine to the organic compound* (symbolized by I_2/R, where R represents the organic compound) in Figures (4.2) to (4.8).

A common feature of the data is that the EMF at high iodine concentrations reaches a plateau at 680 ± 3 mv. This value is equal, within experimental limits, to the EMF value for the formation of silver iodide from pure solid silver and iodine using the same type of cell. Therefore this plateau indicates that elemental iodine is present.

The electrochemical behavior of the various iodine complexes is quite diverse.

In the case of the triphenylphosphine—iodine complex in Figure (4.2). The EMF rises steeply with increasing iodine content to an I_2/R ratio of approximately 1 and then more slowly to the saturation value of 4.3.

The behavior of triphenylamine and 2,4,6-tri(2-pyridyl)-1,3,5-triazine in Figure (4.3) is fairly similar. The EMF values gradually increased as the saturation values of 4.5 and 3.1 for triphenylamine and 2,4,6-tri(2-pyridyl)-1,3,5-triazine, respectively, were approached.

For the compounds, 2,4,6-triphenyl-1,3,5-triazine and1,3,5-Triphenyl benzene, the EMF values are essentially independent of the I_2/R ratio and are close to 680 mv as shown in Figure (4.4). The most likely explanation is that these compounds do not form a complex with iodine. This conclusion is supported by the results of the vapor uptake experiments to be discussed

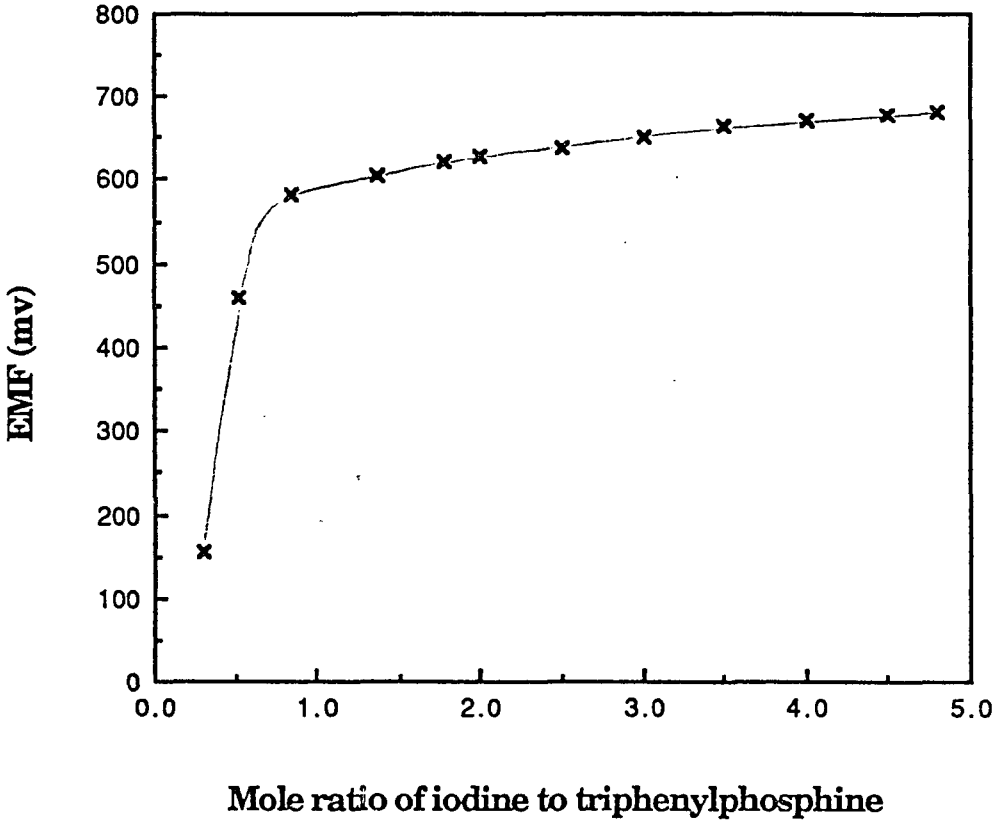

Figure (4.2): EMF curve for triphenylphosphine-iodine

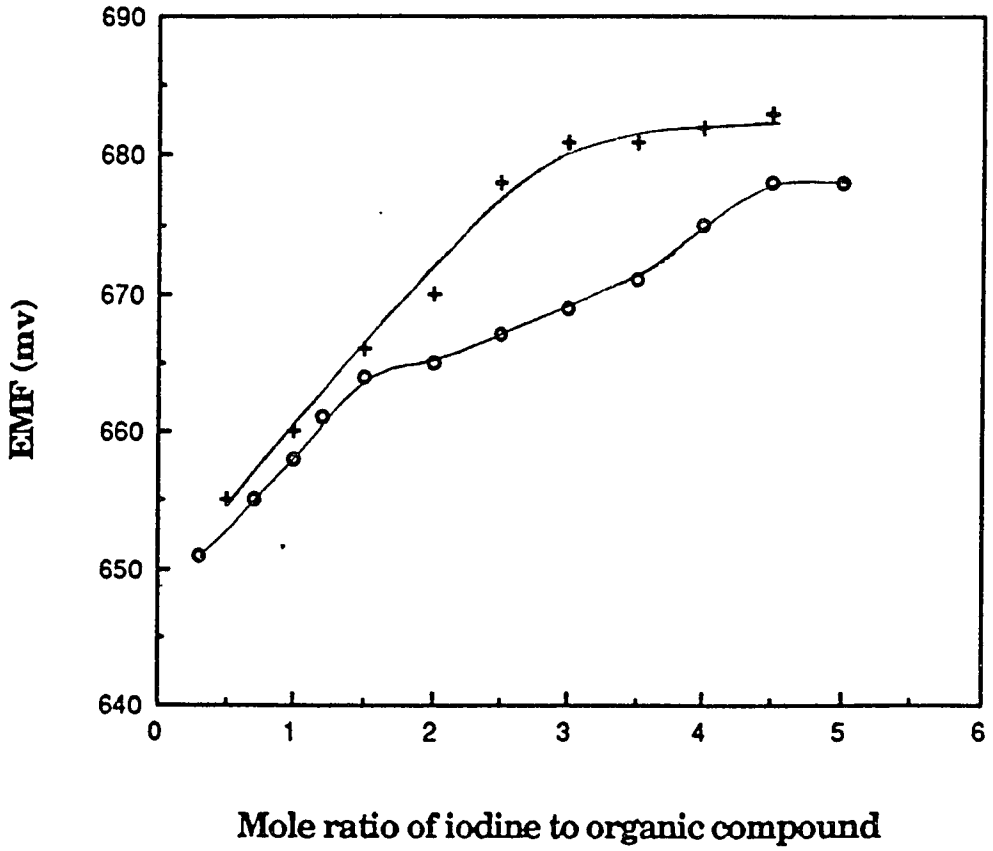

Figure (4.3): EMF curve for ∘, $(Ph)_3N\text{-}I_2$; +, $(PhN)_3(PhN_3)\text{-}I_2$.

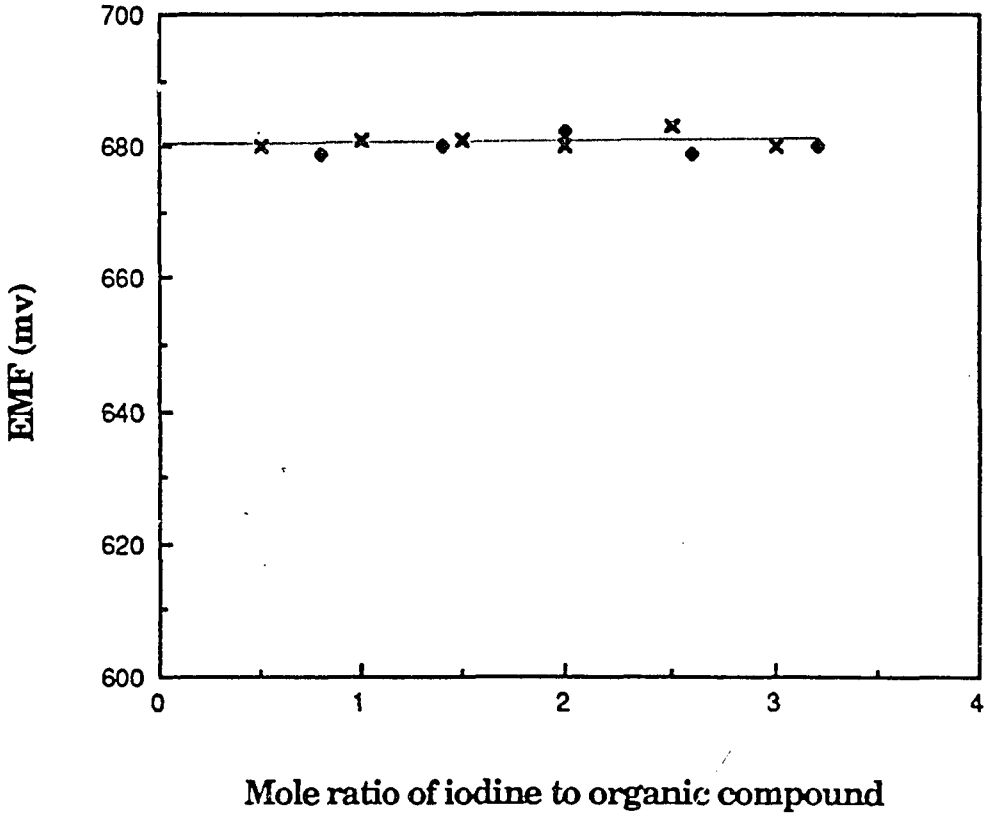

Figure (4.4): EMF curve for ×, Ph_3Ph; ♦, $Ph_3(PhN_3)$

later.

The most interesting behavior is exhibited by the triphenylstibine—iodine complex in Figure (4.5). Up to an I_2/R ratio of 1.5, a solid material is visually observed. From an I_2/R ratio of 1.5 to 3.5, a mixture of solid and liquid is present which corresponds to the appearance of a horizontal plateau in the EMF data. Between 3.5 and the saturation value of 5.7, the material is liquid. Above 5.7, we have a mixture of elemental iodine and liquid material. It is obvious that triphenylstibine forms a liquid complex with iodine and a phase change seems to be occurring at the I_2/R ratio of about 3.8. It might be well to note that triphenylstibine has the lowest melting point of all these compounds, 52-54°C. The presence of a liquid in the iodine complex at room temperature may have some relation to this fact.

In the case of the arsenic compound in Figure(4.6), a phase change seems to be occurring at an I_2 ratio of 3.8.

EMF data for the antimony complex below an I_2/R ratio of 1.0 and for the arsenic complex below a ratio of 2.0 are not presented because the values were not reproducible. This may be related to the fact that the electrical conductivity of these complexes is very low, as discussed in the next chapter, resulting in an irreversible behavior in electrochemical cells.

In the cases of the acridine and phenazine—iodine complexes, each of the EMF curves shows two plateaus in Figures (4.7) and (4.8). In light of the phase rule, each plateau corresponds to a heterogeneous system composed of two phases. The lower plateau at smaller I_2/R ratios represents a mixture of pure solid organic compound and an organic—iodine complex, $R(I_2)_\alpha$, with a constant composition, α, of 1.5 for acridine or 1.0 for phenazine. The upper plateau consists of the organic complex, $R(I_2)_\alpha$, and pure molecular iodine.

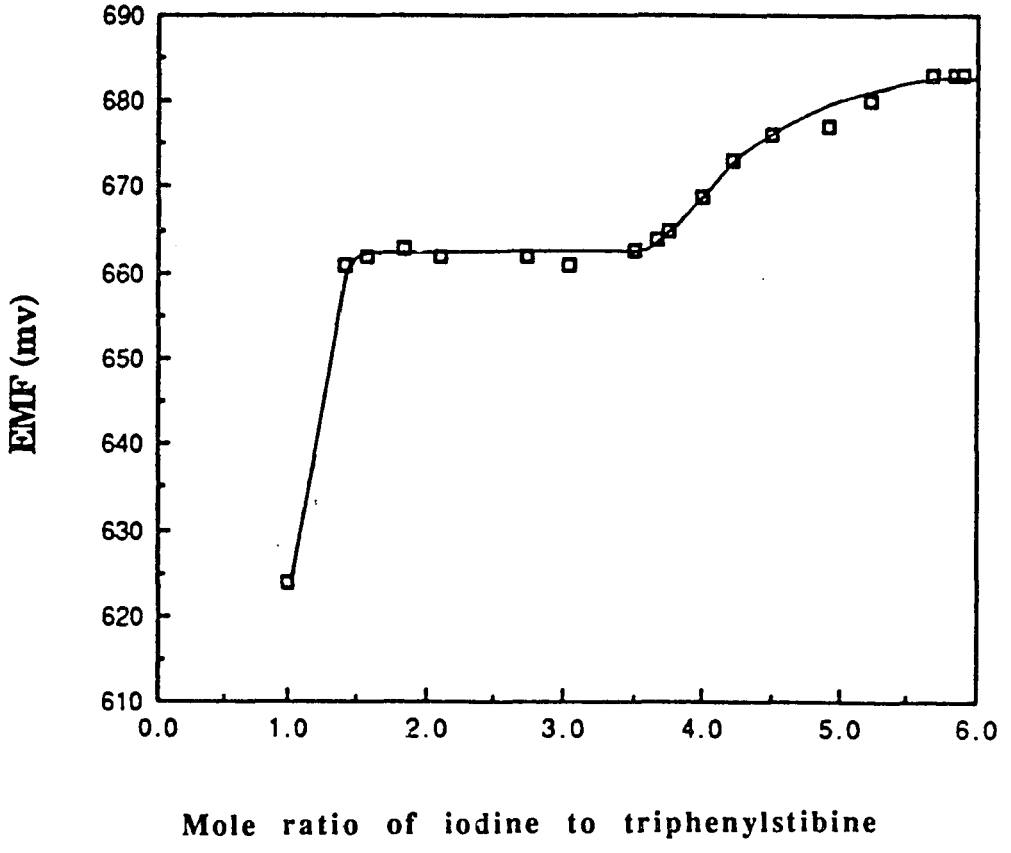

Figure (4.5): EMF curve for triphenylstibine-iodine

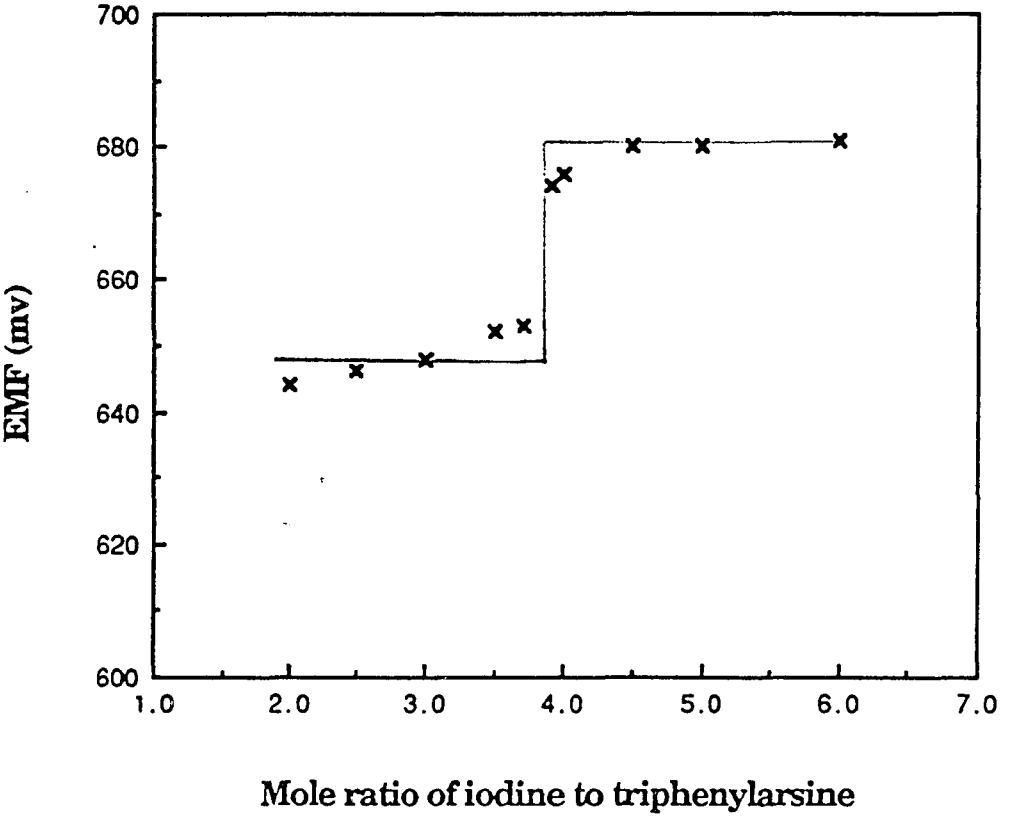

Figure (4.6): EMF curve for triphenylarsine-iodine

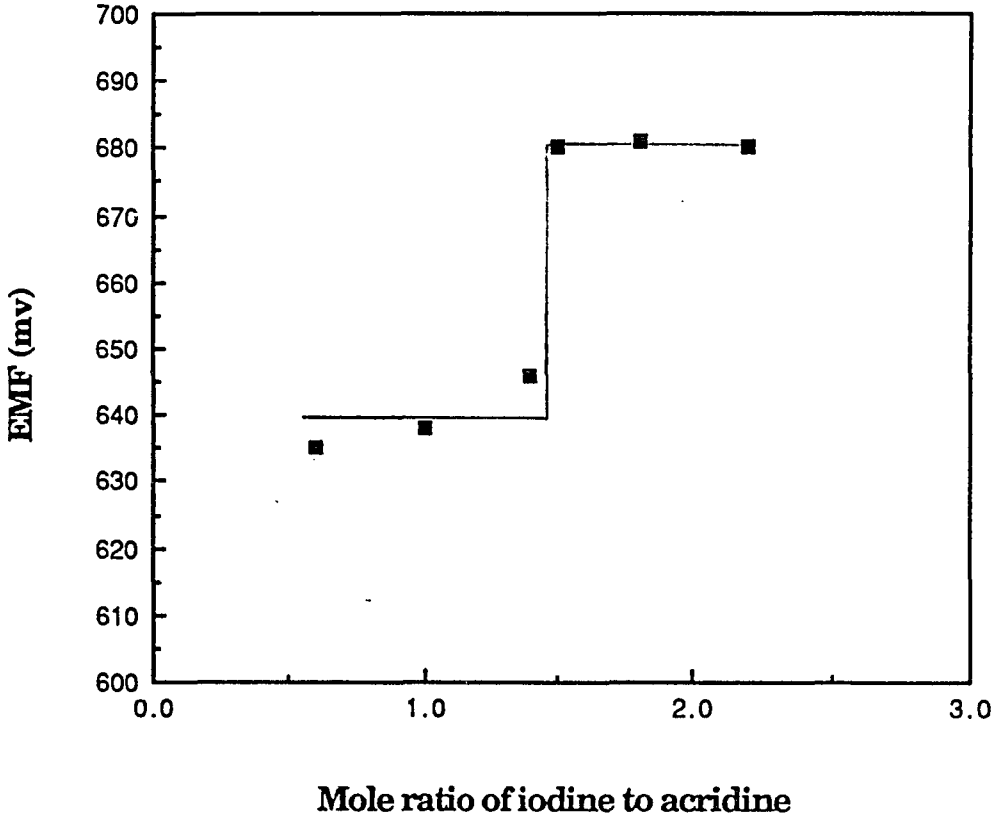

Figure (4.7): EMF curve for acridine-iodine

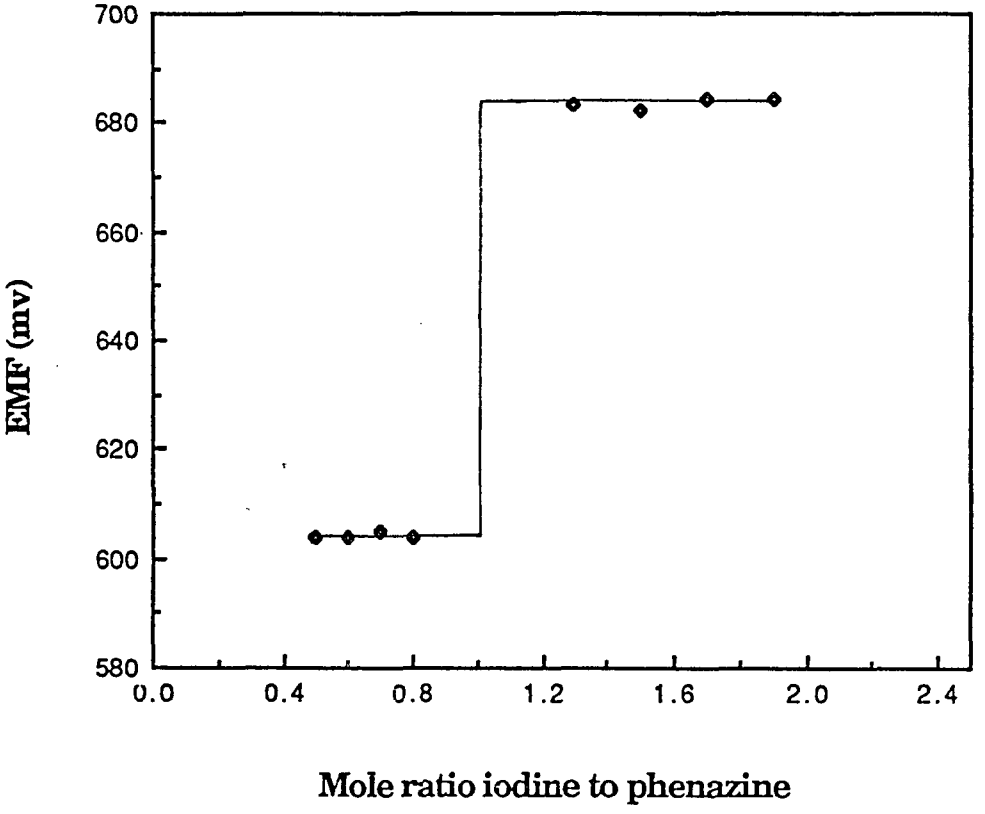

Figure (4.8): EMF curve for phenazine-iodine

4.2-2 Maximum Compositions of Iodine in the Complexes

Maximum compositions of iodine in the complexes were determined by the measurement of maximum vapor absorption of iodine by the organic compounds. Based on the preceding discussion, the maximum composition should correspond, in an EMF curve, to the I_2/R ratio at the point where the last plateau begins.

The maximum absorptions determined from vapor uptake and from the EMF measurements are compared in Table (4-I). The agreement between the two methods is satisfactory. On the basis of this agreement, it seems reasonable to assume that thermodynamically reversible data are being obtained from the EMF measurements.

Upon exposure to iodine vapor at either room temperature or 80°C for several days, both 2,4,6-triphenyl-1,3,5-triazine and 1,3,5-Triphenyl benzene do not absorb iodine. It is evident from the results of both the vapor uptake and EMF measurements that these two triphenyl compounds do not react with iodine.

4.2-3 Calculations of Free Energy of Complex Formation

By means of EMF measurements, Gibbs free energy of formation of iodine complexes can be determined using electrochemical cells of the type:

$$\begin{matrix} (-) & & (+) \\ Pt \mid Ag \mid AgI \mid I_2 \mid Pt & & \langle I \rangle \end{matrix}$$

$$Pt \mid Ag \mid AgI \mid R(I_2)_\alpha \mid Pt \qquad \langle II \rangle$$

In cell I, I_2 refers to pure solid iodine. The EMF of the cell corresponds to the full cell reaction:

$$2Ag + I_2 = 2\ AgI \qquad (4.2\text{-}1)$$

Table 4-I Maximum I_2 compositions determined from vapor uptake and the EMF measurements

Compound	Maximum I_2/R mole ratio	
	vapor uptake	EMF method
$(Ph)_3P$	4.1	4.3
$(Ph)_3As$	3.7	3.8
$(Ph)_3Sb$	5.9	5.7
$(Ph)_3N$	4.5	4.5
$(PhN)_3(PhN_3)$	3.1	3.0
$(Ph)_3(PhN_3)$	no reaction	
$(Ph)_3Ph_3$	no reaction	
$C_{12}H_8N_2$	1.0	1.0
$C_{10}H_6N_4$	1.4	1.5

Ag^+ ions formed at the Ag-AgI interface diffuse through the electrolyte, AgI, and combine with I^- at the AgI-I_2 interface to form AgI. For the transfer of 2 moles of electrons, the free energy of formation of AgI can be determined from cell I by the equation:

$$-2E_I{}^\circ F = 2\bar{G}^\circ_{AgI} - 2\bar{G}^\circ_{Ag} - \bar{G}^\circ_{I_2} \qquad (4.2\text{-}2)$$

where $E_I{}^\circ$ is the EMF value measured for cell I.

In cell II, for a complex of composition, $R(I_2)_\alpha$, the nominal half cell reactions are

$$2Ag - 2e = 2Ag^+ \qquad (4.2\text{-}3)$$

$$\tfrac{1}{\delta} R(I_2)_\alpha + 2e = \tfrac{1}{\delta} R(I_2)_{\alpha-\delta} + 2I^- \qquad (4.2\text{-}4)$$

The full-cell reaction is

$$2Ag + \tfrac{1}{\delta} R(I_2)_\alpha = 2AgI + \tfrac{1}{\delta} R(I_2)_{\alpha-\delta} \qquad (4.2\text{-}5)$$

δ is an infinitesimally small number, and the concentration change is therefore negligible. The free energy change of this reaction, which corresponds to the EMF value of cell II, is

$$-2E_{II}{}^\circ F = 2\bar{G}^\circ_{AgI} + \tfrac{1}{\delta}\bar{G}^\circ_{R(I_2)_{\alpha-\delta}} - 2\bar{G}^\circ_{Ag} - \tfrac{1}{\delta}\bar{G}^\circ_{R(I_2)_\alpha} \qquad (4.2\text{-}6)$$

Subtracting the two chemical equations, Eq.(4.2-5) from Eq.(4.2-1), yields the reaction:

$$R(I_2)_{\alpha-\delta} + \delta I_2 = R(I_2)_\alpha \qquad (4.2\text{-}7)$$

Thus, subtracting the corresponding free energies, Eq.(4.2-6) from Eq.(4.2-2), we obtain *the free energy change per mole of iodine in this re-*

action, $\Delta_\delta\bar{G}^0$:

$$\Delta_\delta\bar{G}^\circ = -2(E_I^\circ - E_{II}^\circ)F = {}^1\!/\!_\delta\,\bar{G}^\circ_{R(I_2)_\alpha} - {}^1\!/\!_\delta\,\bar{G}^\circ_{R(I_2)_{\alpha-\delta}} - \bar{G}^\circ_{I_2} \quad (4.2\text{-}8)$$

The partial molar free energy of the complexes can be expressed in the following equations:

$$\bar{G}^\circ_{R(I_2)_\alpha} = \bar{G}_{I_2}[R(I_2)_\alpha] + \bar{G}_R[R(I_2)_\alpha] \quad (4.2\text{-}9)$$

$$\bar{G}^\circ_{R(I_2)_{\alpha-\delta}} = (\alpha-\delta)\bar{G}_{I_2}[R(I_2)_{\alpha-\delta}] + \bar{G}_R[R(I_2)_{\alpha-\delta}] \quad (4.2\text{-}10)$$

in which *the partial molar free energy*, $\bar{G}_{I_2}[R(I_2)_\alpha]$ or $\bar{G}_R[R(I_2)_\alpha]$, is essentially a constant through its infinitesimally narrow range, δ. Therefore Eq.(4.2-10) can be rewritten as:

$$\bar{G}_{R(I_2)_{\alpha-\delta}} = (\alpha - \delta)\bar{G}_{I_2}[R(I_2)_\alpha] + \bar{G}_R[R(I_2)_\alpha] \quad (4.2\text{-}11)$$

Substituting Eq.(4.2-11) and Eq.(4.2-9) into Eq.(4.2-8), we have:

$$\Delta_\delta\bar{G}^0 = -2F(E_I^0 - E_{II}^0) = \bar{G}_{I_2}[R(I_2)_\alpha] - \bar{G}^0_{I_2} \quad (4.2\text{-}12)$$

Eq. (4.2-12) automatically manifests a conclusion that $\Delta_\delta\bar{G}^0$ is equal to *the relative partial molar free energy of iodine* $\Delta_\alpha\bar{G}_{I_2}$:

$$\Delta_\delta\bar{G}^0 = \Delta_\alpha\bar{G}_{I_2} \quad (4.2\text{-}13)$$

which is the difference between the partial molar free energy of iodine in the complex $R(I_2)_\alpha$ and the molar free energy of pure iodine, corresponding to the reaction:

$$I_2(s) = I_2[R(I_2)_\alpha] \qquad (4.2\text{-}14)$$

It is feasible, (see §.2-6), to deduce the molar free energy of formation of the charge-transfer complex $R(I_2)_\alpha$ as a function of $\Delta_\alpha\bar{G}_{I_2}$:

$$\Delta\bar{G}^0 = \left(\frac{1-X_{I_2}'}{X_{I_2}'}\right)\int_0^{X_{I_2}'} \frac{\Delta_\alpha\bar{G}_{I_2}}{(1-X_{I_2})^2}\, dX_{I_2} \qquad (4.2\text{-}15)$$

where X_{I_2} is the mole fraction of iodine, X_{I_2}' is the mole fraction of iodine at the composition selected for calculating a $\Delta\bar{G}^0$ value[25].

Inspection of the EMF curves reveals that two cases are possible:

1. $(E_I^\circ - E_{II}^\circ)$ is a constant between 0 and α which is a plateau in the EMF curve corresponding to a heterogeneous system containing two phases. Based on Eqs.(4.2-12), (4.2-13) and (4.2-15), the free energy of formation of the complex $R(I_2)_\alpha$ per mole of iodine, $\Delta\bar{G}^0$, can then be calculated from the difference of EMF values of cell I and cell II:

$$\Delta\bar{G}^0 = -2F(E_I^0 - E_{II}^0) \qquad (4.2\text{-}16)$$

2. The value of $(E_I^\circ - E_{II}^\circ)$ is a function of iodine composition, a solid solution exists between the composition from 0 to α. In this case, $\Delta\bar{G}^0$, can be calculated by numerical integration of the expression from Eqs.(4.2-12), (4.2-13) and (4.2-15):

$$\Delta\bar{G}^{0} = \left(\frac{1-X_{I_2}'}{X_{I_2}'}\right)\int_0^{X_{I_2}'} \frac{2F(E_I^0-E_{II}^0)}{(1-X_{I_2})^2}\, dX_{I_2} \qquad (4.2\text{-}17)$$

Since the integration must start at $X_{I_2} = 0$, all the data were extrapolated to an I_2/R ratio of 0.

4.2-4 Discussion of Free Energy of Complex Formation

Free energies of formation of the complexes at the maximum I_2/R ratios are listed in Table(4-II). The uncertainties in ΔG° are higher for the triphenylarsine and triphenylstibine because of the larger range of extrapolation to an I_2/R ratio of 0. Entropy and enthalpy values were not obtained because the experimental data were not accurate enough to obtain precise values of the temperature dependence of the EMF.

Based on the fact that entropy values of iodine charge-transfer complexes are very similar and relatively small[13], we will discuss the experimental results on the assumption that the free energy can be considered as a measure of the bond strength between iodine and the organic compounds.

Free energies of formation of triphenyl group VA—iodine complexes at an I_2/R ratio of 3.8 are listed in Table(4-III), as well as the relative partial molar free energies of iodine for an I_2/R ratio of 2.0. It is observed that the order of absolute values of the free energy of formation of the iodine complexes is P > As > Sb > N.

The phosphorous complex, with the most negative free energy values,produces the strongest bonding. The nitrogen complex yields the weakest bonding in the group. We may attribute the difference to a two-way donor-acceptor action. Nitrogen can have no function other than a simple

Table 4-II **Free energies of formation of iodine complexes at maximum compositions**

Formation of iodine complexes	$-\Delta G$ (KJ/mol I_2) at maximum I_2/R mole ratio
$(Ph)_3P + 4.3I_2 = (Ph)_3P \cdot (I_2)_{4.3}$	25.0 ± 2
$(Ph)_3As + 3.8I_2 = (Ph)_3As \cdot (I_2)_{3.8}$	7.9 ± 4
$(Ph)_3Sb + 5.8I_2 = (Ph)_3Sb \cdot (I_2)_{5.8}$	5.9 ± 4
$(Ph)_3N + 4.5I_2 = (Ph)_3N \cdot (I_2)_{4.5}$	3.3 ± 2
$(PhN)_3(PhN_3) + 3.1I_2 = (PhN)_3(PhN_3) \cdot (I_2)_{3.1}$	3.8 ± 2
$(Ph)_3(PhN_3)$	no reaction
$(Ph)_3Ph_3$	no reaction
$C_{12}H_8N_2 + 1.0I_2 = (C_{12}H_8N_2) \cdot I_2$	15.6 ± 1
$C_{10}H_6N_4 + 1.5I_2 = (C_{10}H_6N_4) \cdot (I_2)_{1.5}$	8.5 ± 2

Table 4-III

Free energy values for iodine complexes of triphenyl group VA compounds at selected compositions

Compound	$-[\overline{G}I_2(c) - \overline{G}^*I_2]$ (KJ/mol I_2) at I_2/R mole ratio 2.0	$-\Delta G$ (KJ/mol I_2) at I_2/R mole ratio 3.8
$(Ph)_3P$	12.5 ± 0.8	31.0 ± 2
$(Ph)_3As$	7.1 ± 0.8	7.9 ± 4
$(Ph)_3Sb$	4.1 ± 0.4	7.9 ± 4
$(Ph)_3N$	3.3 ± 0.8	4.1 ± 2

n-donation, because no other orbital is accessible. P, As and Sb in the triphenyl compounds can function as acceptors with low-lying $d\pi$ orbitals as well as n-donors.

It is not surprising that $(Ph)_3P$ is considered to be a good two-way donor. Presumably the possibility of intramolecular dative conjugation between the phenyl rings and $d\pi$ orbitals of P enhances the $d\pi$-acceptor capacity of the phosphorus atom. However the reason why P is the strongest one among P, As and Sb remains unknown[14]. The x-ray studies of these compounds[26,27] did not give evidence of any significant difference in the structures of $(Ph)_3P$, $(Ph)_3As$ and $(Ph)_3Sb$, either. Nevertheless, the result we have obtained here is the same as that obtained for the heat of reaction of triphenyl compounds with boron trihalides[28] P < As < Sb. The donor ability of complexes of P, As and Sb also decreases in the order P > As > Sb[15].

A comparison of free energies of nitrogen-bearing aromatic compounds, shown in Table(4-IV), suggests that nitrogen atoms present in a molecule do not necessarily guarantee that a complex will form. $(Ph)_3(PhN_3)$ has three nitrogens, yet forms no complex with iodine. $(Ph)_3N$ contains much less nitrogen than $(PhN)_3(PhN_3)$, but forms a stable complex. These results support Mulliken's point[14] that the geometric approachability could be a dominant factor in donor-acceptor interactions.

Based on the fact that $(Ph)_3Ph$ does not absorb iodine, it is safe to say that, in these compounds, the π-electron delocalization over each single aromatic rings is not sufficient to lead to a donor-acceptor interaction with iodine. Hence, the nitrogens are the only species which act as electron donors. Furthermore, it is possible that the approachability of iodine to the nitrogens in these compounds dictates the extent to which a charge-transfer reaction will take place. The vanishing of the donor ability of nitrogens in $(Ph)_3(PhN_3)$ may result from a steric effect because the outer three phenyl groups are isolating the nitrogens in the central ring from iodine. This

Table 4-IV

Free energy values for iodine complexes of nitrogen-bearing aromatic compounds at selected compositions

Compound	$-[\overline{G}I_2(c) - \overline{G}^*I_2]$ (KJ/mol I_2) at I_2/R mole ratio 2.0	$-\Delta G$ (KJ/mol I_2) at I_2/R mole ratio 3.0
$(Ph)_3N$	3.3 ± 0.8	4.8 ± 2
$(PhN)_3(PhN_3)$	2.6 ± 0.8	3.9 ± 2
$(Ph)_3(PhN_3)$	no reaction	
$(Ph)_3Ph$	no reaction	

should also be the case for the three nitrogens on the central ring of $(PhN)_3(PhN_3)$. The fact that $(Ph)_3N$ forms a stronger complex with iodine than $(PhN)_3PhN_3$ implies that the nitrogen at the top of the $(Ph)_3N$ pyramid may have a larger exposed surface than the nitrogens in the terminal rings of $(PhN)_3(PhN_3)$. Undoubtedly, to obtain better information about the importance of steric hindrance, intensive studies of the structures of well-crystallized molecular complexes are necessary.

Acridine and phenazine, in which steric hindrance is negligible, manifest a difference in the bond strengths with iodine which simply results from the different number of nitrogens in the molecules. In Table (4-V) below, it is observed that the free energy of formation for the phenazine-iodine complex is a little less than double that for the acridine-iodine complex. Nitrogen atoms are known to act as electron donors. The two condensed aromatic rings, in these system, may have charge density donation as well. However, it is obvious that the enhanced thermodynamic stability of phenazine-iodine over acridine-iodine is attributable to the presence of the extra nitrogen.

§.4-3 Electrical Conductivity

4.3-1 Variation of Conductivity With Iodine Content

Electrical conductivity measurements were made on the iodine complexes. The conductivities of the solid iodine complexes of triphenylphosphine, -arsine, -stibine, as well as acridine and phenazine, were low, $<10^{-5}(\Omega cm)^{-1}$,and not reproducible from sample to sample. The conductivities of the solid complexes of $(Ph)_3N$ and $(PhN)_3(PhN_3)$ and the liquid complex of $(Ph)_3Sb$ were measured at 25°C. The variations in their conductivities with iodine content are shown in Figure(4.9). The logarithms of the conductivities

Table 4-V

Free energy values for iodine complexes of acridine and phenazine at a selected composition

Compound	$-[E_{I_2}(c) - E^*_{I_2}]$ (mv) at I_2/R mole ratio 1.0	$-\Delta G$ (KJ/mol I_2) at I_2/R mole ratio 1.0
$C_{12}H_8N_2$	81	15.6 ± 1
$C_{10}H_6N_4$	43	8.5 ± 2

are plotted against moles of iodine per mole of organic molecule.

All the above organic materials themselves do not conduct electricity. Iodine is also an insulator. However, when some organic compounds interact with iodine, the resulting complexes have semiconducting properties. This observation may be explained by means of the band theory. The interaction between two insulators, a completely filled valence band of the donor — organic molecule and the empty conduction band of the acceptor — iodine, brings their electronic states together, while the electron density is transferred from the donor to acceptor. As a result of the charge-transfer process, partially filled bands are formed in complex formation which results in electrical conduction. (§.2.5-1)

It was observed that, for $(Ph)_3N$, $(PhN)_3(PhN_3)$ and $(Ph)_3Sb$, the conductivity does not strongly depend on the iodine content and the liquid complex has a higher conductivity than the solid ones.

Similar to studies[29] on iodine and bromine complexes in some other systems, the results of our studies on thermodynamic stability and conductivity conform to the fact that high thermodynamic stability, in general, is associated with low conductivity. $(Ph)_3N$ and $(PhN)_3(PhN_3)$ form relatively weaker solid iodine complexes in the system, but are better conductors. Other organic compounds, such as $(Ph)_3P$, $(Ph)_3As$ and phenazine, form stronger complexes with iodine, but they have lower conductivities. $(Ph)_3Sb\text{-}I_2$ may be an exception, but it forms a liquid complex.

4.3-2 Temperature Dependence of the Conductivities

The temperature dependence of the conductivities of $(Ph)_3N$ and $(Ph)_3Sb$ complexes is shown in Figure(4.10). Assuming that the equation

$$\sigma = \sigma_0 \exp(-\frac{E_a}{RT}) \qquad (2.5\text{-}5)$$

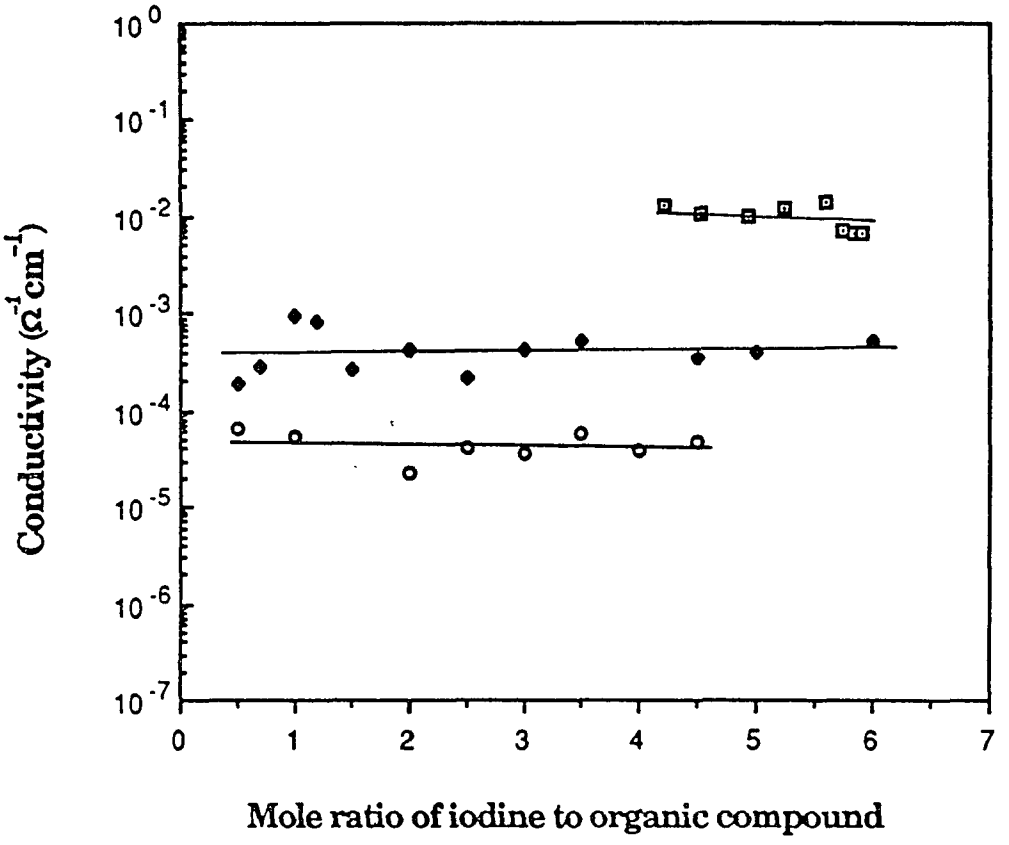

Figure (4.9): Variation of conductivity with iodine content:
○, $(PhN_3)_3(PhN_3)$; ◆, $(Ph)_3N$; ▫, $(Ph)_3Sb$ (liquid).

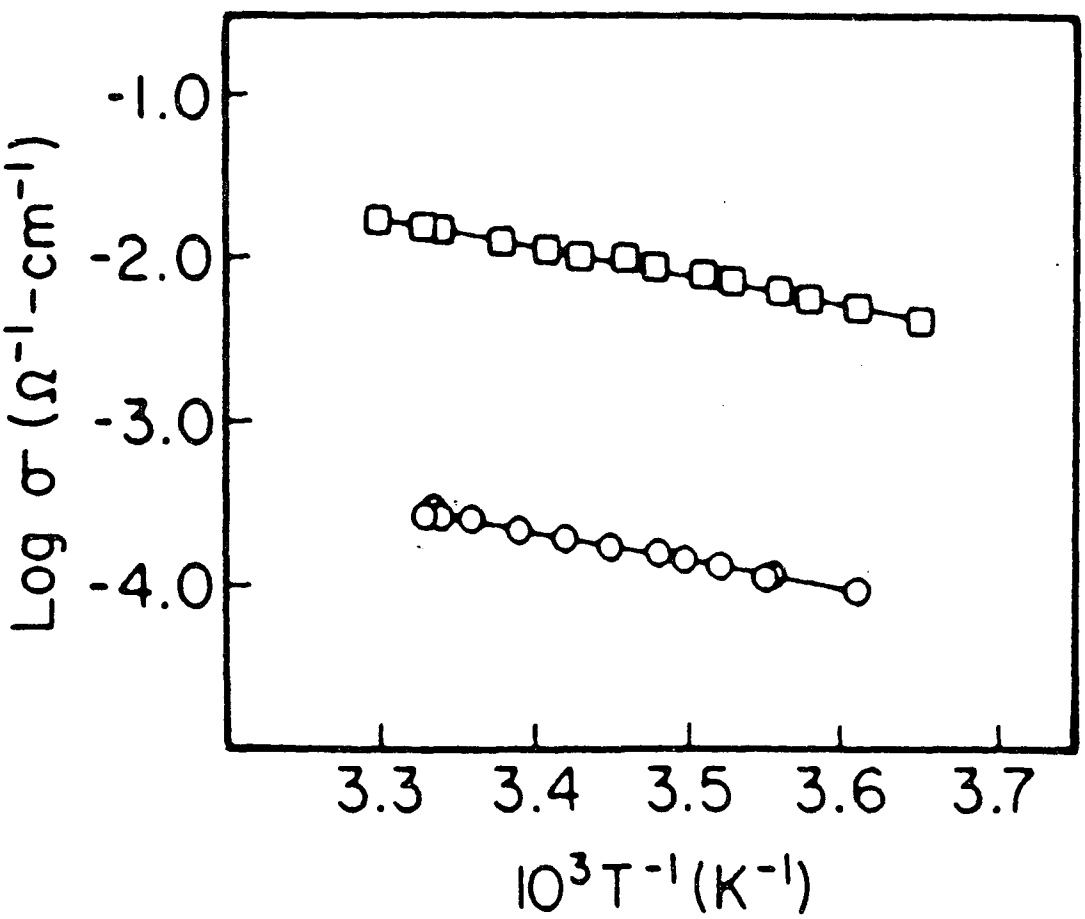

Figure (4.10): Temperature dependence of the conductivity: o, $(Ph)_3N(I_2)_{4.0}$; □, $(Ph)_3Sb(I_2)_{5.80}$ (liquid).

applies, activation energies of 0.34 and 0.32 ev were calculated for the solid complex $(Ph)_3N(I_2)_{4.0}$ and the liquid complex $(Ph)_3Sb(I_2)_{5.8}$ respectively.

4.3-3 Conduction Mechanism of the Iodine Complexes

In the study of the conductivity of liquid Sb complex, we observed that ac and dc measurements on the Sb complex yielded identical results. This indicates that there is a significant electronic contribution to the conductivity.

In an attempt to determine whether the conduction is ionic or electronic in the solid iodine complexes, a further electrochemical experiment[29] was performed. The electrochemical cell<1> and cell<2>, shown below, were prepared and their EMFs were measured as E_1 and E_2, respectively. Combining cell<1> and cell<2>, we constructed cell<3> whose EMF was determined as E_{exp}.

$$Pt \mid Ag \mid AgI \mid R(I_2)_x \mid Pt \qquad <1>$$

$$Pt \mid Ag \mid AgI \mid R(I_2)_y \mid Pt \qquad <2>$$

$$Pt \mid Ag \mid AgI \mid R(I_2)_x \mid R(I_2)_y \mid AgI \mid Ag \mid Pt \qquad <3>$$

$$(x < y)$$

By comparing the value of E_{exp} with (E_1-E_2), we can determine the percentage of the ionic or electronic conduction in the complexes.

Consider a virtual electrolysis resulting from the passage of 2 moles of electrons through cell<3> as follows.

Figure(4.11) shows a transport process in a complex which has 100% electronic conduction. On the left side of the cell, Ag^+ ions gain 2 moles of

$$\overset{2e\Rightarrow}{\mathbf{Pt}} \mid \mathbf{Ag} \mid \mathbf{AgI} \mid \mathbf{R(I_2)_x} \mid \mathbf{R(I_2)_y} \mid \mathbf{AgI} \mid \mathbf{Ag} \mid \mathbf{Pt} \overset{2e\Rightarrow}{}$$

$$\overset{\Leftarrow Ag^+ \; I^- \Rightarrow}{} \qquad \overset{I^- \Rightarrow \; \Leftarrow Ag^+}{}$$

$$2Ag^+ + 2e = 2Ag \qquad 2Ag - 2e = 2Ag^+$$

$$\tfrac{1}{\delta} R(I_2)_x + 2I^- - 2e = \tfrac{1}{\delta} R(I_2)_{x+\delta} \qquad \tfrac{1}{\delta} R(I_2)_y + 2e = \tfrac{1}{\delta} R(I_2)_{y-\delta} + 2I^-$$

$$2\,AgI + \tfrac{1}{\delta} R(I_2)_x = \tfrac{1}{\delta} R(I_2)_{x+\delta} + 2Ag \qquad 2Ag + \tfrac{1}{\delta} R(I_2)_y = 2AgI + \tfrac{1}{\delta} R(I_2)_{y-\delta}$$

$$\tfrac{1}{\delta}\,\mathbf{R(I_2)_x} + \tfrac{1}{\delta}\,\mathbf{R(I_2)_y} = \tfrac{1}{\delta}\,\mathbf{R(I_2)_{x+\delta}} + \tfrac{1}{\delta}\,\mathbf{R(I_2)_{y-\delta}}$$

$$\Delta_\delta G^\circ = -2FE_{ele}, \quad E_{ele} = E_{II} - E_I = E_{exp}, \quad \frac{E_{exp}}{E_{ele}} = 1$$

Figure (4.11): 100% Electronic Conduction in Complexes

electrons forming Ag at the Ag-AgI interface. I^- ions diffuse through the AgI to react with $R(I_2)_x$ at the AgI-$R(I_2)_x$ interface. 2 moles of electrons are released to the right side of the cell. On the right, the Ag releases 2 moles of electrons to form Ag^+ ions at the Ag-AgI interface which, then, diffuse through the AgI and combine with I^- ions produced by $R(I_2)_y$ at the interface of the two complexes.

The above analysis of the transport process leads to the following expression for the overall reaction in cell<3>:

$$\frac{1}{\delta} R(I_2)_x + \frac{1}{\delta} R(I_2)_y = \frac{1}{\delta} R(I_2)_{x+\delta} + \frac{1}{\delta} R(I_2)_{y-\delta} \qquad (4.3\text{-}1)$$

where δ is the change in iodine content. It is clear that Eq.(4.3-1) is a combination of the two cell reactions whose EMF's are represented by E_1 and E_2. Therefore, the observed EMF for the complexes with 100% electronic conduction, E_{ele}, is equal to the difference in the EMF's of cell<1> and cell<2>:

$$E_{ele} = E_2 - E_1 \qquad (4.3\text{-}2)$$

A mole of iodine is transferred from $R(I_2)_x$ to $R(I_2)_y$ and the corresponding free energy is given by the equation:

$$\Delta_\delta G^\circ = -2FE_{ele} \qquad (4.3\text{-}3)$$

In the case of a 100% ionic conduction of complexes shown in Figure (4.12), no I_2 is transferred and the measured EMF would be zero, since no free energy change occurs. The transport process is merely a transfer of AgI from the left side to the right side in cell<3>.

Thus, the experimental voltage measured for cell<3>, E_{exp}, is attributed to the electronic conduction in the complexes. It readily follows that the fraction of electronic conduction in the overall conduction mechanism can

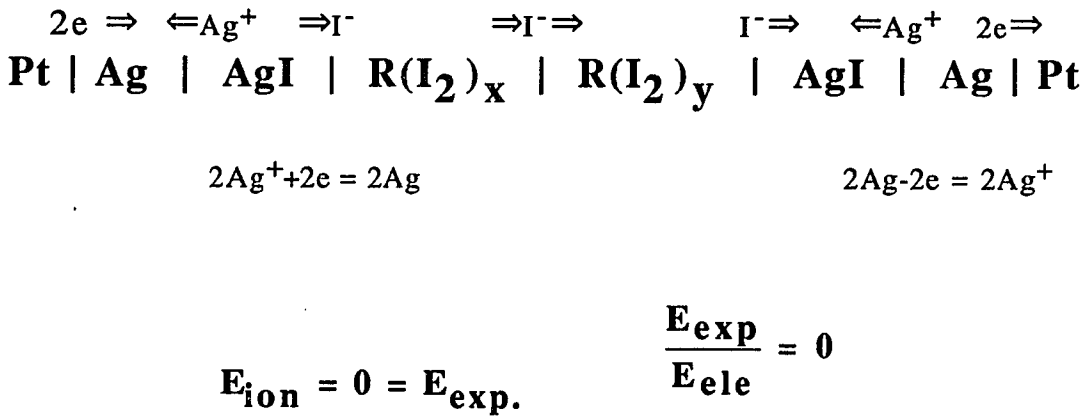

Figure (4.12): 100% Ionic Conduction in Complexes

be expressed by the ratio of the measured EMF, E_{exp}, to the maximum possible EMF, E_{ele} or (E_2-E_1), which is represented by the electron transport number, t_{ele}:

$$t_{ele} = \frac{E_{exp}}{E_{ele}} = 1 \text{ to } 0 \qquad (4.3\text{-}4)$$

We have used this technique on the iodine-triphenyl complexes. The results are presented in Table(4-VI). The fact that the value of E_{exp} is very close to the E_{ele} value in each case, within experimental error, is a good evidence that conduction in these complexes is primarily electronic.

Table(4-VI) Comparsion of the experimental voltage, Eexp. and the calculated volatage, Eele.=(E_{II}-E_I)

Complex	Composition(x)	EMF(mv)	Eele.(mv)	Eexp.(mv)
$Ph_3N(I_2)_x$	3.0	667		
			12	11
	1.0	655		
			20	21
	4.5	675		
$Ph_3P(I_2)_x$	3.0	640		
			58	60
	0.85	582		
			46	47
	2.0	628		
$Ph_3As(I_2)_x$	4.0	672		
			31	31
	2.0	641		
$Ph_3Sb(I_2)_x$	5.9(Liq.)	682		
			82	82
	1.0(Sol.)	600		
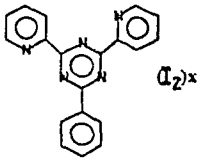	4.0	682	12	12
	2.0	670		
	1.5	658	12	11
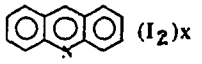	1.8	681		
			60	61
	0.6	621		

Chapter 5 IONIC DISSOCIATION MECHANISMS IN ORGANIC SOLUTION

Several spectroscopic studies and conductance measurements[5,6] have demonstrated that significant ionization of the iodine complexes of triphenyl group VA compounds and pyridine occurs in polar organic solvents.

In this chapter, several different ionization mechanisms for the complexes in 1,2-dichloroethane(DCE) are proposed, depending on the chemical nature of the organic molecules and concentration ratios of the reactants. Many reaction sequences and ionization mechanisms were considered. Those presented here were found to be in best accord with the experimental data.

The term "nominal concentration" used in connection with I_2, Ph_3As, Ph_3Sb, Py and TEAI refers to the number of moles added to a liter of DCE solution. Dissociation and interaction in solution are not considered. The symbol used for nominal concentrations is 'c' as in $c(I_2)$ and $c(Ph_3As)$. The actual concentrations are shown in brackets as in $[I_3^-]$ and $[Ph_3AsI_2]$.

§.5-1 High Concentration Ratios of Iodine to Organic Molecules

Reaction Mechanism

The following reaction scheme was used for high concentration ratios of iodine to organic molecule in 1,2-dichloroethane.

$$R + I_2 \longrightarrow RI_2 \qquad (5\text{-}1)$$

$$RI_2 + I_2 \rightleftarrows RI^+ + I_3^- \qquad (5\text{-}2)$$

$$RI^+ + 2I_2 \rightleftarrows RI_2^{2+} + I_3^- \qquad (5\text{-}3)$$

We assume that the addition of tetraethylammonium iodide results quantitatively in the following reaction.

$$I_2 + TEAI \longrightarrow I_3^- + TEA^+ \qquad (5\text{-}4)$$

R in the reactions represents the organic molecule. We assume that reaction (5-1) proceeds completely to the right* and that sufficient time has elapsed so that the complex present is the inner complex, RI^+I^-, which, for convenience, we write as RI_2. The extent to which reactions (5-2) and (5-3) proceed to the right depends on the nature of the organic molecule and the concentration ratio of the reactants. It would be quite complicated to quantitatively study all the equilibria in these ionization reactions, if the system simultaneously involved more than one equilibrium. Fortunately, the EMF and conductivity data obtained in our study show that, for pyridine and triphenylamine, reaction(5-2) is the only ionic dissociation reaction of the iodine complexes. For the other organic molecules, solutions with sufficiently high concentration ratios of iodine to organic compound can be prepared so that reaction(5-2) essentially proceeds to completion and reaction(5-3) becomes the only equilibrium reaction operating.

A further assumption, that concentrations can be substituted for thermodynamic activities, permits us to write the following expressions for the equilibrium constants.

$$K_2 = \frac{[RI^+][I_3^-]}{[RI_2][I_2]} \qquad (5\text{-}5)$$

$$K_3 = \frac{[RI_2^{2+}][I_3^-]}{[RI^+][I_2]^2} \qquad (5\text{-}6)$$

---

* : A disproportionation constant, K, for $I_3^- = I_2 + I^-$ was reported[30 31] in pyridine to be 1.25×10^{-5} M.

Complexes of the form RI^+ have been proposed by many investigators. A new complex, RI_2^{2+}, is being proposed by us on the basis of the experimental data to be presented below. The Lewis structures of the ions are shown in Figure (5.1).

For electrochemical cells of the type:

$$\underset{(a)}{Pt \mid R, I_2} \parallel \underset{(b)}{R, I_2, TEAI \mid Pt} \qquad (5\text{-}7)$$

where the nominal concentrations of R and I_2 are the same on both sides of the cell, we propose the following virtual electrochemical reactions at the platinum electrodes.

$$3I_2(a) + 2e = 2I_3^-(a) \qquad (5\text{-}8)$$

$$2I_3^-(b) - 2e = 3I_2(b) \qquad (5\text{-}9)$$

The species in solution are in equilibrium, so the choice of electrode reactions is somewhat arbitrary. Species should be selected which are in reasonably high concentration in the solution such as I_2 and I_3^-. The selection of a different pair of electrode reactions will give the same results as long as they are in accord with the equilibria specified in reactions (5-2) and (5-3).

The EMF of such a cell is

$$E = -\frac{RT}{2F} \ln \frac{[I_3^-(a)]^2 [I_2(b)]^3}{[I_3^-(b)]^2 [I_2(a)]^3} \qquad (5\text{-}10)$$

The mathematical treatment used to obtain values for K_2 and K_3 is discussed in appendix A.

(M = N, P, As or Sb.)

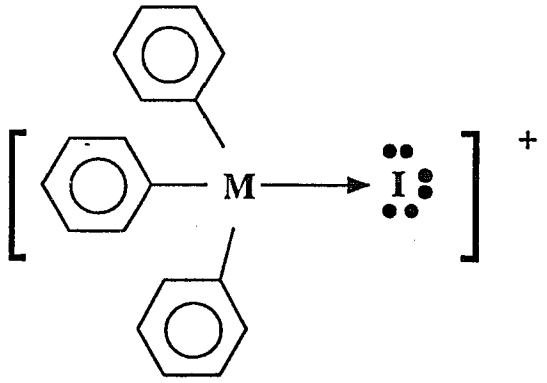

RI^{+}

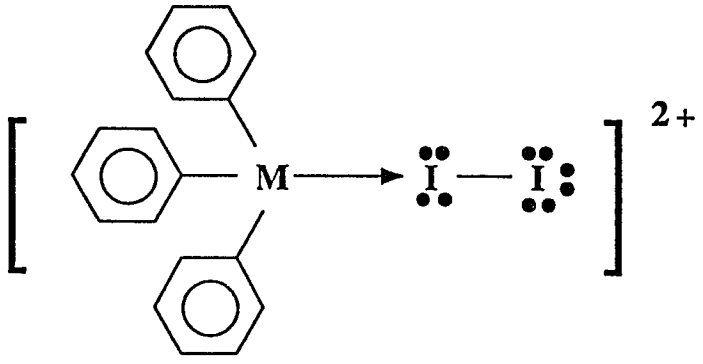

RI_2^{2+}

Figure (5.1): Lewis structures of the ions

5.1-1 Iodine Complexes of Pyridine and Triphenylamine

A simple, approximate treatment can be performed using data at high iodine concentrations if the only equilibrium reaction of importance is reaction (5-2). Such a treatment appears to be appropriate for pyridine and triphenylamine-iodine reactions. If enough TEAI is added on side b in line-diagram (5-7), the assumption can be made that reaction (5-2) is completely suppressed and that the concentration of I_3^- on side b is the nominal concentration of TEAI according to reaction (5-4). An approximate form of equation (5-10) can then be used.

$$E \approx -\frac{RT}{F} \ln \frac{[I_3^-(a)]}{[I_3^-(b)]} \approx -\frac{RT}{F} \ln \frac{[I_3^-(a)]}{c(TEAI)} \qquad (5\text{-}11)$$

where $[I_3^-(a)]$ is the concentration of I_3^- for the intrinsic dissociation of the complex according to reaction (5-2).

Data obtained for pyridine and triphenylamine at various iodine concentrations are shown in Table (5-I) and Table (5-III), respectively. For pyridine complex, the dissociation calculated using equation (5-11) increases from 18 per cent to 57 per cent as we go from a $c(I_2)$ /c(Py) ratio of 25 to 200. For triphenylamine complex, the dissociation increases from 3.9 per cent to 56 per cent as the $c(I_2)/c(Ph_3N)$ ratio goes from 10 to 150. In both cases, the data below an iodine to organic molecule ratio of 100 do not yield a constant value for the equilibrium constant, K_2. The most probable reason for this is that the assumption that reaction (5-1) proceeds all the way to the right is not applicable at lower ratios.

In Table (5-II) and (5-IV) are EMF data on the interactions of iodine with pyridine and triphenylamine, respectively, which were used to calculate the equilibrium constants for reaction (5-2). Equations (5-2) and (5-5) and the mathematical treatment in Appendix A1 were used in this analysis. By computer calculation, using trial values of K_2 and successive

Table (5-I) Dependence of the ionic dissociation of the pyridine-iodine complex on the concentrations of iodine

$c(Py) = 1.00 \times 10^{-3}$ M, $c(TEAI) = 3.00 \times 10^{-3}$ M

$\frac{c(I_2)}{c(Py)}$	EMF (mv)	$\frac{[I_3^-]}{c(Py)}$
25	72.6	0.18
50	59.6	0.29
75	54.8	0.35
100	48.0	0.46
200	—	0.57*

* This value was calculated from the data in Table (5-II).

Table (5-II) EMF values for pyridine-iodine solution at high iodine concentrations*

c(Py) ($M \times 10^3$)	c(TEAI) ($M \times 10^3$)	EMF exp. (mv)	EMF calc. (mv)
2.00	0.400	7.5	6.7
2.00	1.00	11.6	11.1
2.00	1.40	15.5	15.1
2.00	2.00	25.2	25.8
1.00	0.400	10.9	10.7
1.00	1.00	21.5	22.3
1.00	1.40	26.1	28.2
1.00	2.00	31.5	35.4

* The nominal iodine concentration in all these measurements was 0.200 M. The equilibrium constant, K_2, used to calculate the EMF values was 3.9×10^{-3}.

Table (5-III)

Dependence of the ionic dissociation of triphenylamine-iodine complex on the concentrations of iodine

$c(Ph_3N) = 1.50 \times 10^{-3}$ M, $c(TEAI) = 3.00 \times 10^{-3}$ M

$\frac{c(I_2)}{c(Ph_3N)}$	EMF (mv)	$\frac{[I_3^-]}{c(Ph_3N)}$
10	100.9	0.039
30	76.9	0.10
60	56.1	0.22
100	—	0.49*
150	—	0.56*

* This value was calculated from the data in Table (5-IV).

Table (5-IV) EMF values for triphenylamine-iodine solutions at high iodine concentrations*

$c(I_2)$ (M x 10)	c(TEAI) (M x 10^3)	EMF exp. (mv)	EMF calc. (mv)
1.50	0.455	9.5	9.3
1.50	0.833	16.0	15.5
1.50	1.15	19.6	20.1
1.50	1.43	23.0	23.6
2.25	1.50	20.4	22.5
2.25	3.00	31.7	35.5

* The nominal Ph_3N concentration in all these measurements was 1.50×10^{-3} M. The equilibrium constant, K_2, used to calculate the EMF values was **4.8×10^{-3}**.

approximations (see Appendix A1), a value of K_2 was selected which best fit the experimental EMF data. The value selected for pyridine was 3.9×10^{-3} and 4.8×10^{-3} for triphenylamine. On the basis of the sensitivity of the calculated EMF values to the choice of the equilibrium constant, the error in K_2 and the other equilibrium constants to be discussed is estimated to be within ± 50 per cent.

A check on the validity of the results for pyridine presented in Table (5-I) and Table (5-II) was made by comparing the electrical conductivity of a solution containing nominal concentrations of 2.0×10^{-1}M I_2 and 1.0×10^{-3}M TEAI with the conductivity of a solution with nominal concentrations of 2.0×10^{-1}M I_2 and 1.0×10^{-3}M Py. The conductivity values, 2.7×10^{-4} $(\text{ohm-cm})^{-1}$ and 1.4×10^{-4} $(\text{ohm-cm})^{-1}$ respectively, are shown in Table (5-V). The I_3^- concentrations for the two solutions are calculated to be 1.0×10^{-3} M and 0.57×10^{-3}M respectively on the basis of equations (5-4) and (5-2). If we make the crude assumption that the ionic conductivities of TEA^+ and PyI^+ are equal, the ratio of the conductivity ratio, 0.52, is in reasonable agreement with the concentration ratio, 0.57.

Reasonable agreement was also shown in a similar comparison for triphenylamine-iodine complex. The results are listed in Table (5-V) to be 0.41 and 0.49 for the ion concentration ratio and electrical conductivity ratio, respectively.

5.1-2 Iodine Complexes of Triphenylstibine, -arsine and -phosphine

As we have discussed, for pyridine and triphenylamine, the agree

Table (5-V)

Conductivities of solutions at high iodine concentrations

Compound R	c(R) Mx10^3	c(I_2) Mx10^3	conductivity $(\Omega\cdot cm)^{-1}x10^4$	(ratio)	$[I_3^-]$ Mx10^3	(ratio)
Py	1.00	200	1.4		0.57	
				0.52		0.57
TEAI	1.00	200	2.7		1.00	
Ph_3N	1.50	150	1.7		0.74	
				0.41		0.49
TEAI	1.50	150	4.1		1.50	
Ph_3Sb	1.00	100	3.2		1.19	
				1.07		1.19
TEAI	1.00	100	3.0		1.00	
Ph_3As	1.50	150	3.9		1.92	
				0.93		1.28
TEAI	1.50	150	4.2		1.50	
Ph_3P	1.50	75	3.7		1.56	
				0.90		1.04
TEAI	1.50	75	4.1		1.50	

ment between the experimental EMF readings and the calculated EMF data in Table (5-II) and Table (5-IV) shows that the iodine complexes are dissociated into RI^+ and I_3^- according to reaction (5-2). However, the experimental data obtained for iodine complexes of Ph_3Sb, Ph_3As and Ph_3P do not fit this one step ionization mechanism.

Experimental EMF data for triphenyl group VA compounds are plotted against the mole ratio of iodine to organic molecule in Figure (5.2). Compared with the iodine complex of Ph_3N, more I_3^- was produced from the complexes of Ph_3P, Ph_3As and Ph_3Sb in accord with the lower experimental values of the EMF.

The remarkable difference in behavior also appears in the variation in the electrical conductivity. As shown in Figure (5.3), the conductivities of Ph_3P, Ph_3As and Ph_3Sb differ from that of Ph_3N, increasing steeply with increasing iodine concentration and then reaching horizontal plateaus of higher conductivities at much lower mole ratios of I_2/R. (That the Ph_3Sb curve parts from that of Ph_3P and Ph_3As in Figure (5.3) is due to the lower concentration of Ph_3Sb.) The rapidly increasing and higher conductivities of the iodine complexes of Ph_3P, Ph_3As and Ph_3Sb may indicate easier formation of inner complexes and more extensive dissociation of the complexes.

Therefore, an additional ionization step, reaction (5-3), which postulates the existence of a new complex ion, RI_2^{2+}, was invoked. The assumptions were made that reaction (5-1) and reaction (5-2) proceed completely to the right and that the equilibrium process in reaction (5-3) is in operation.

In Table (VI), (VII) and (VIII) are EMF data on the interaction between iodine and Ph_3Sb, Ph_3As and Ph_3P which were used to calculate the equilibrium constant, K_3. Equations (5-3) and (5-6) and the treatment in Appendix A2 were used in this analysis. The values of K_3 which best fit the

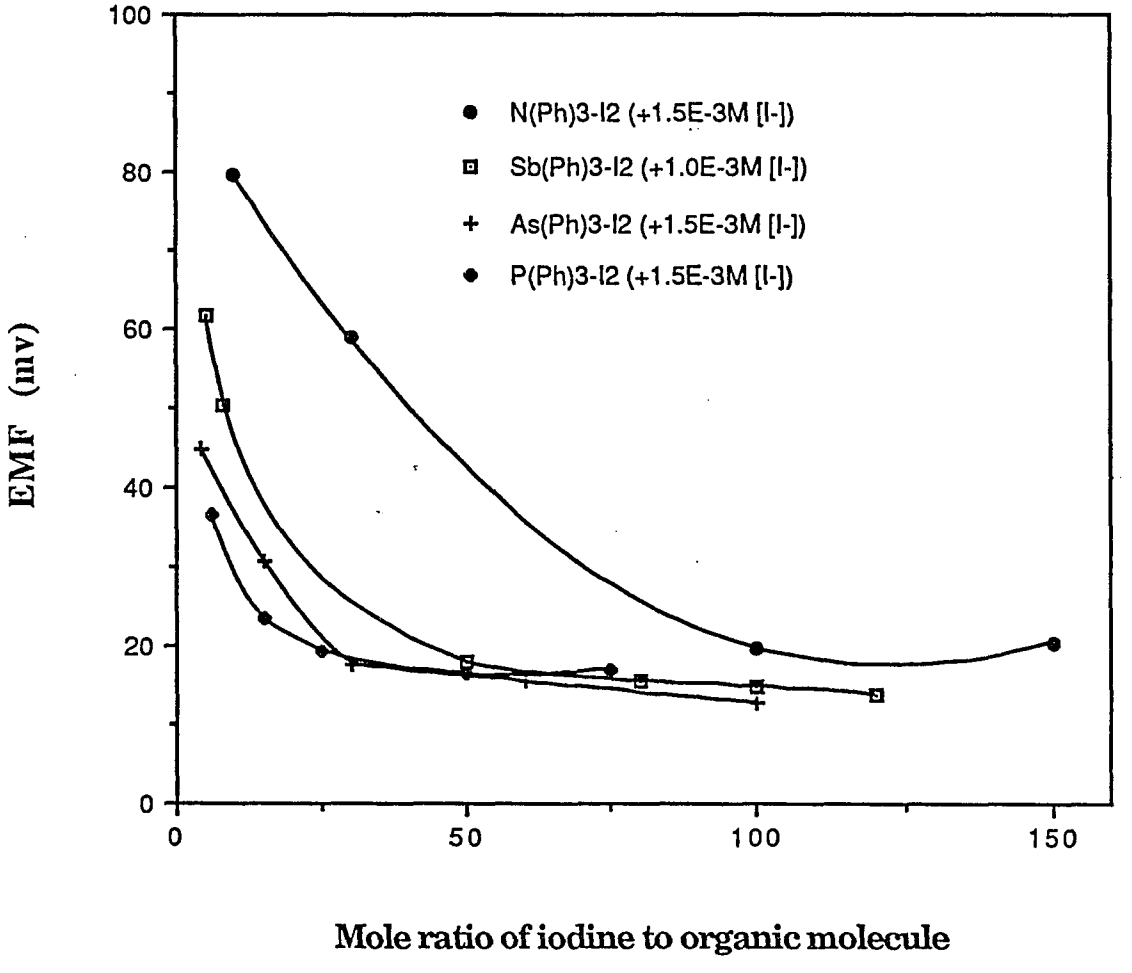

Figure (5.2): Variation of EMF with iodine content

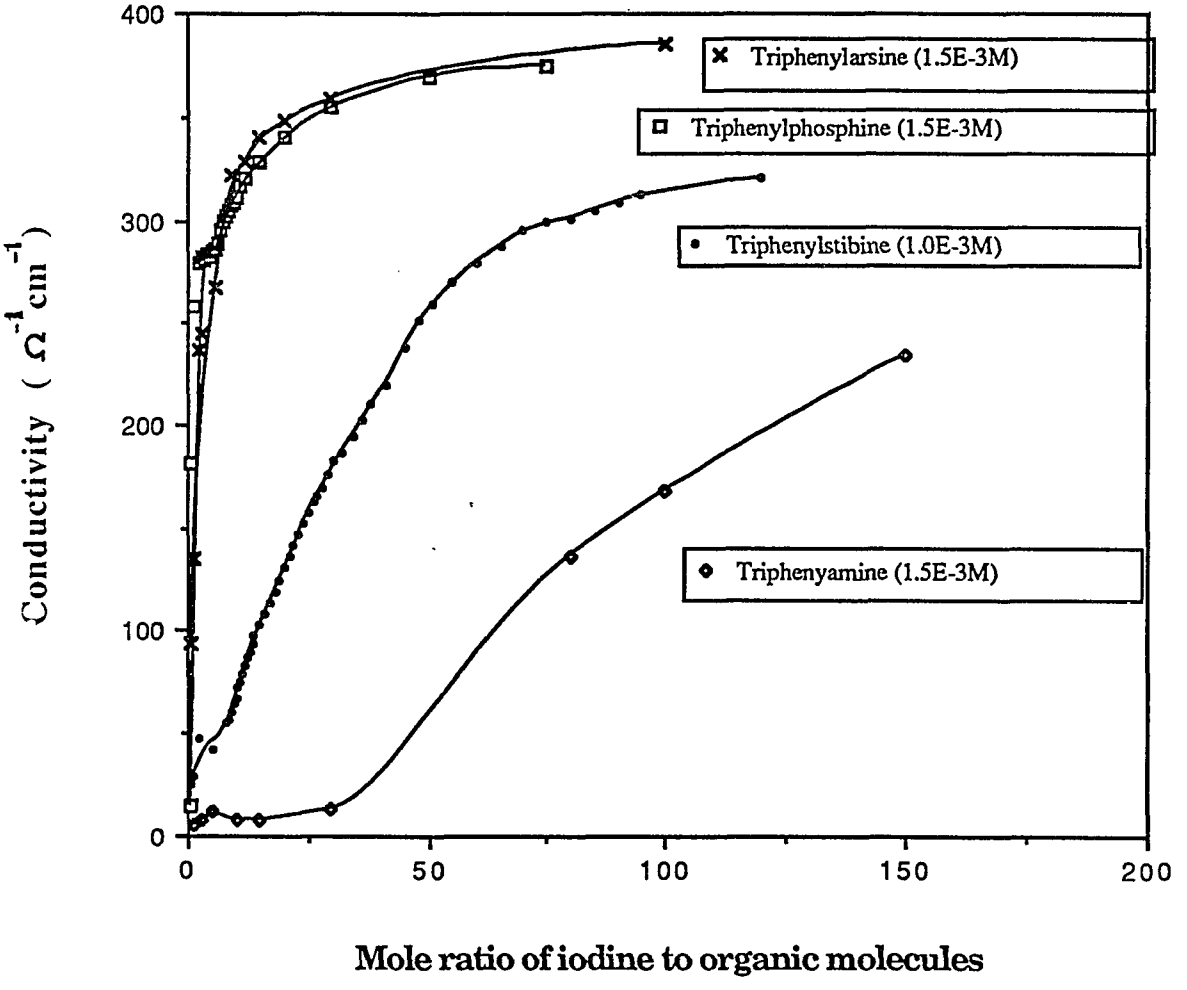

Figure (5.3): Variation of conductivity with I_2/R ratio

Table (5-VI) EMF values for Ph_3Sb-iodine solutions at high iodine concentrations*

$c(I_2)$ (M x 10)	c(TEAI) (M x 10^3)	EMF exp. (mv)	EMF calc. (mv)
1.20	0.200	4.4	3.4
1.20	0.500	8.0	7.9
1.20	0.700	10.6	10.5
1.20	1.00	13.9	14.1
1.00	0.200	4.1	3.6
1.00	0.500	8.3	8.3
1.00	0.700	10.9	11.1
1.00	1.00	14.8	14.8
0.800	0.200	4.2	3.8
0.800	0.500	8.7	8.8
0.800	0.700	11.9	11.7
0.800	1.00	15.5	15.5
0.500	0.200	5.0	4.3
0.500	0.500	11.4	9.6
0.500	0.700	14.3	12.7
0.500	1.00	17.8	16.8

* The nominal Ph_3Sb concentration in all these measurements was 1.00×10^{-3} M. The equilibrium constant, K_3, used to calculate the EMF values was $2.9 \times 10^{-2}\ M^{-1}$.

Table (5-VII) EMF values for Ph_3As-iodine solutions at high iodine concentrations*

$c(I_2)$ (M x10)	c(TEAI) (M x 10^3)	EMF exp. (mv)	EMF calc. (mv)
1.50	0.500	5.4	5.2
1.50	0.750	7.5	7.5
1.50	1.50	12.7	13.5
1.50	3.00	22.7	22.7
0.900	0.500	6.2	6.1
0.900	0.750	9.0	8.7
0.900	1.50	15.4	15.4
0.900	3.00	25.6	25.2
0.450	0.500	7.0	6.9
0.450	0.750	9.8	9.8
0.450	3.00	17.6	17.0
0.450	3.00	29.8	27.3

* The nominal Ph_3As concentration in all these measurements was 1.50×10^{-3} M. The equilibrium constant, K_3, used to calculate the EMF values was **3.8×10^{-2} M^{-1}**.

Table (5-VIII) EMF values for Ph_3P-iodine solutions at high iodine concentrations*

$c(I_2)$ ($M \times 10^{-1}$)	c(TEAI) ($M \times 10^{3}$)	EMF exp. (mv)	EMF calc. (mv)
1.13	0.500	7.0	6.6
1.13	0.750	8.6	9.3
1.13	1.50	17.0	16.3
1.13	3.00	26.5	26.4
0.75	0.500	6.8	7.0
0.75	0.750	9.4	9.9
0.75	1.50	16.4	17.0
0.75	3.00	27.6	27.3
0.38	0.500	8.4	7.3
0.38	0.750	11.0	10.3
0.38	1.50	19.3	17.6
0.38	3.00	33.1	27.9

* The nominal Ph_3P concentration in all these measurements was 1.50×10^{-3} M. The equilibrium constant, K_3, used to calculate the EMF values was $\mathbf{1.2 \times 10^{-2}\ M^{-1}}$.

data were 2.9 x 10^{-2} M^{-1}, 3.8 x $10^{-2}M^{-1}$ and 1.2 x $10^{-2}M^{-1}$ respectively for Ph_3Sb, Ph_3As and Ph_3P.

EMF measurements were also made for solutions with lower concentration ratios of iodine to organic molecules. However, it was found that, when the nominal concentration ratios of iodine to organic molecule are smaller, a constant value for K_3 could not be obtained. This may be because at lower ratios the assumption that reaction (5-2) proceeds completely to the right is not applicable. Both equilibrium processes in reactions (5-2) and (5-3) may be in operation. As shown in Table (5-VIII) for Ph_3P, for instance, at a concentration ratio of 25, the calculated and experimental EMF data start to diverge.

A comparison of conductivity data was made at high concentration ratios of I_2/R as shown in Table (5-V). The I_3^- concentration values were calculated using the selected values of the equilibrium constant, K_3. The comparison is more complex than in the case of pyridine and triphenylamine because of the presence of the two ionic species, Ph_3MI^+ and $Ph_3MI_2^{2+}$. The agreement between the conductivity ratios and the I_3^- concentration ratios is not as good as in the case of pyridine and Ph_3N especially for Ph_3As. The conductivity data do, at least qualitatively, support the assumption that the complexes are completely ionized at these high concentration ratios of iodine to organic molecule.

We have observed that, at high iodine concentrations, Ph_3Sb, Ph_3As and Ph_3P form the $Ph_3MI_2^{2+}$ ion as well as the Ph_3MI^+ ion whereas Py and Ph_3N only form the PyI^+ ion. Some factors that may play a role in this difference of behavior are the differences in molecular geometry and ionization energy and the presence of empty d orbitals of fairly low energy in the

phosphorus, arsenic and antimony atoms which can result in backbonding. In nitrogen, the possibility of the d-orbital participation in the activated complex does not exist.(§. 2-2)

§.5-2 High Concentration Ratios of Organic Molecules to Iodine

Reaction Mechanisms

The following reaction scheme was used for high concentration ratios of organic molecule to iodine in 1,2-dichloroethane.

$$R + I_2 \longrightarrow RI_2 \qquad (5\text{-}1)$$

$$RI_2 \rightleftarrows RI^+ + I^- \qquad (5\text{-}12)$$

Reaction (5-1) proceeds completely to the right, as evidenced by the absence of the I_2 absorption band (at about 500 nm) in the UV-visible spectrum. The expression for the equilibrium constant corresponding to reaction (5-12) is

$$K=\frac{[RI^+][I^-]}{[RI_2]} \qquad (5\text{-}13)$$

For electrochemical cells of the type in line-diagram (5-7), we propose the following electrode reactions

$$RI^+(a) + 2e = R(a) + I^-(a) \qquad (5\text{-}14)$$

$$R(b) + I^-(b) - 2e = RI^+(b) \qquad (5\text{-}15)$$

The expression for the cell EMF is

$$E = -\frac{RT}{2F} \ln \frac{[R(a)][I^-(a)][RI^+(b)]}{[R(b)][I^-(b)][RI^+(a)]} \qquad (5\text{-}16)$$

The mathematical treatment used to obtain values for K_{12} is discussed in appendix B.

5.2-1 Iodine Complexes of Triphenylarsine and Triphenylphosphine

A previous study[6] on the pyridine-iodine system by Aronson et al indicated that at high concentration ratio of pyridine to iodine the complex is dissociated by the reaction:

$$2RI_2 = R_2I^+ + I_3^- \qquad (5\text{-}17)$$

This does not appear to be the case for the iodine complexes of Ph_3As, Ph_3P and Ph_3Sb on the basis of our electrochemical data and spectrophotometric study. In the case of Ph_3As and Ph_3P, reactions (5-1) and (5-12) are in best agreement with the experimental data at sufficiently high concentration ratio of the organic molecules to iodine. In the case of Ph_3Sb, the electrochemical data obtained could not be fitted with any simple mechanism and will not be discussed further in this thesis.

Triphenylphosphine and triphenylarsine in 1,2-dichloroethane show UV absorption bands at 291 nm and 293 nm,respectively. On addition of iodine to the triphenyl compound, the solution turns yellow and two fairly intense bands at about 290 nm and 365 nm are observed which are characteristic of the triiodide ion. The intensities of the I_3^- bands were found to decrease as the concentration ratios of Ph_3P and Ph_3As to I_2 increased as is shown in Figures (5.4) and (5.5). These results can be interpreted in terms of the following scheme:

$$R + I_2 \longrightarrow RI_2 \qquad (5\text{-}1)$$

$$RI_2 \rightleftarrows RI^+ + I^- \qquad (5\text{-}12)$$

$$RI^+ + 2I^- \rightleftarrows I_3^- + R \qquad (5\text{-}18)$$

The higher the concentration of the organic molecule in the solution, the more reaction (5-18) would proceed to the left, so that less I_3^- is observed in the UV-visible spectrum. We also observed the equilibrium process of reaction (5-18) by adding I^- into Ph_3As-I_2 solution, I_3^- absorbances increased immediately then decreased with time, particularly when the Ph_3As concentration was sufficiently high.

At Ph_3P to I_2 concentration ratios of 10 and above, the solution became colorless very soon after adding I_2 to Ph_3P and no I_3^- was observed spectrophotometrically indicating the absence of I_3^-. In the case of Ph_3As, when the concentration ratio went up to 500 or higher, the I_3^- absorption bands disappeared after the solution reached equilibrium in about a week as determined by conductivity measurements and the solution turning colorless. A probable reason for this difference of behavior is that the phosphorus compound forms a stronger bond with iodine than the arsenic compound. Equilibrium reaction(5-18) more readily to proceeds to the right if the bond between the organic molecule and iodine is weaker.

Electrochemical measurements were made on the colorless solutions at high concentration ratios of organic molecule to iodine. Data obtained on Ph_3As-I_2 and Ph_3P-I_2 solutions are shown in Table (5-IX) and Table (5-X), respectively. Equations (5-12) and (5-13) and the treatment in Appendix B were used to obtain a value for the equilibrium constant, K_{12}. The values selected were 2.4×10^{-5}M and 2.2×10^{-4}M for triphenylarsine and triphenylphosphine, respectively. A comparison of conductivity data with I_2-TEAI solutions was again made as shown in table (5-XI). The I_3^- concentration ratios, 0.13 for Ph_3As and 0.38 for Ph_3P, are reasonably close to their conductivity ratios, 0.12 and 0.50 respectively.

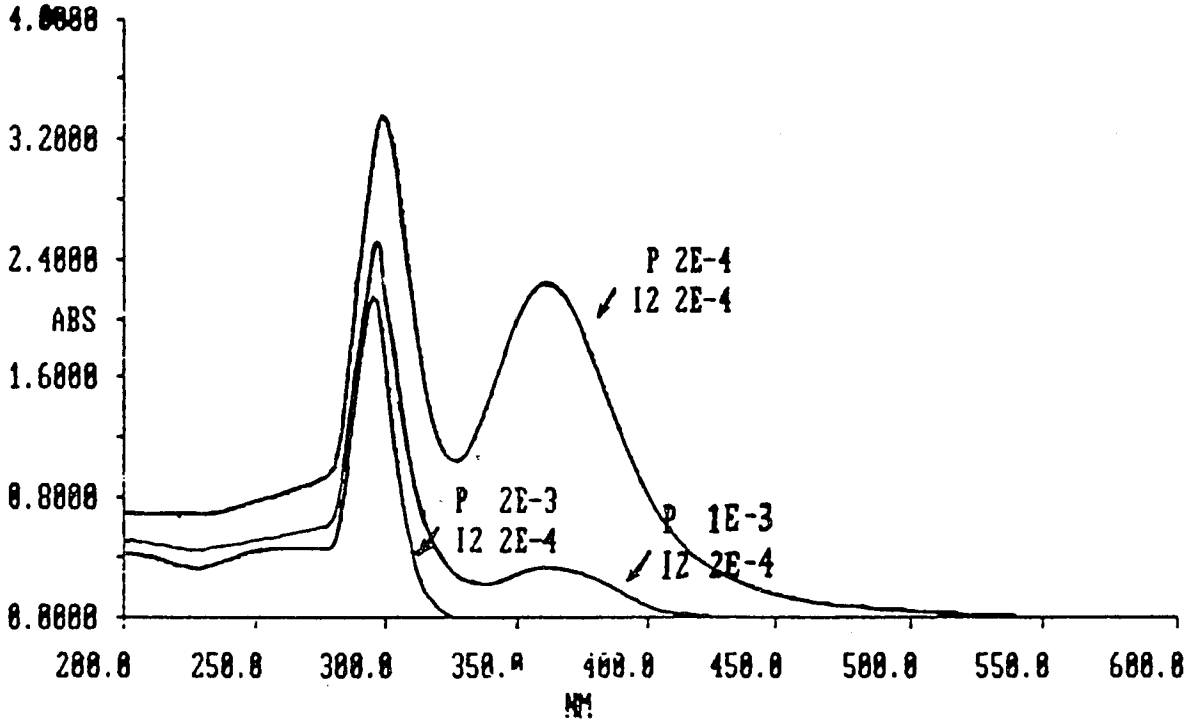

Figure (5.4): UV-visible spectrum of $Ph_3P + I_2$ in 1,2-dichloroethane

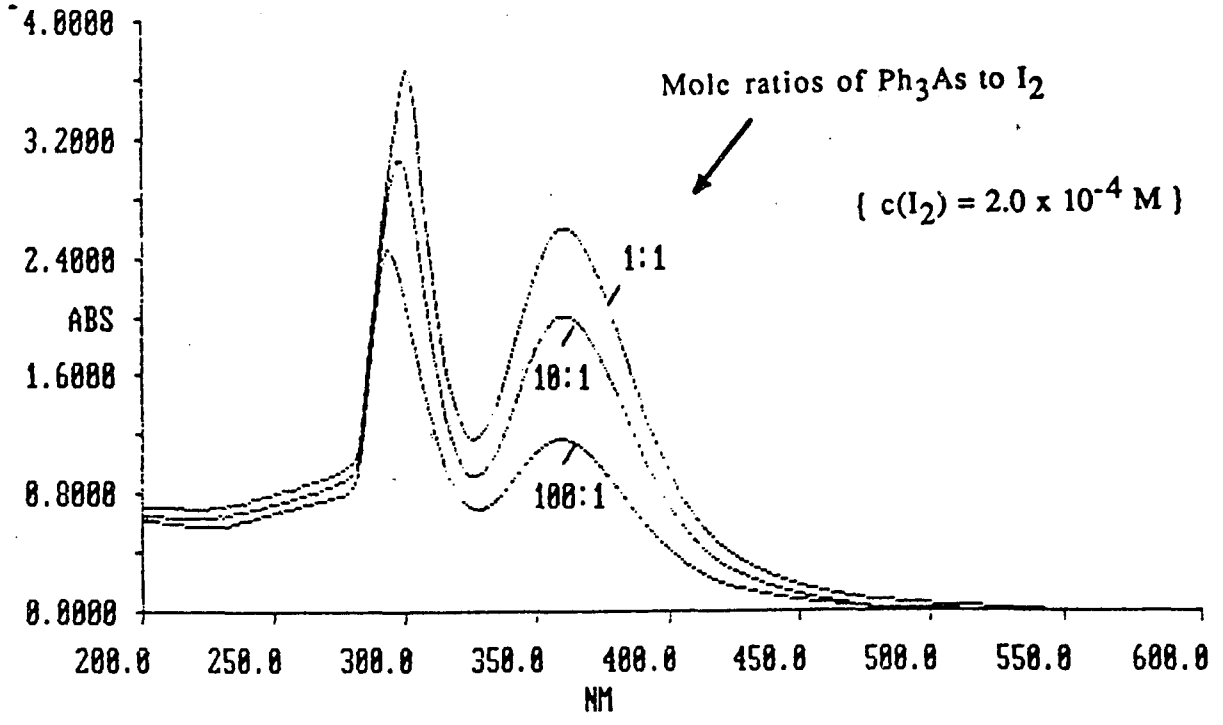

Figure (5.5): UV-visible spectrum of $Ph_3As + I_2$ in 1,2-dichloroethane

Table (5-IX)

EMF values for Ph_3As-iodine solutions at high concentrations of Ph_3As*

c(Ph_3As) (M)	c(I_2) (M x 10^3)	c(TEAI) (M x 10^3)	EMF exp. (mv)	EMF calc. (mv)
0.500	1.00	0.600	36.5	36.7
0.500	1.00	0.900	48.6	46.0
0.500	1.00	1.80	64.1	63.0
0.500	1.00	3.00	75.0	75.9
0.350	0.500	1.00	58.1	57.1
0.350	0.500	2.00	73.3	74.5
0.350	0.500	3.00	82.6	84.8

* The equilibrium constant, K_{12}, used to calculate the EMF values was **2.4 x 10^{-5} M**.

Table (5-X)

EMF values for Ph_3P-iodine solutions at high concentrations of Ph_3P*

$c(Ph_3P)$ ($M \times 10^2$)	$c(I_2)$ ($M \times 10^3$)	c(TEAI) ($M \times 10^3$)	EMF exp. (mv)	EMF calc. (mv)
1.00	1.00	0.100	3.4	3.3
1.00	1.00	0.400	12.0	12.1
1.00	1.00	0.700	19.1	19.3
1.00	1.00	1.00	24.6	25.2
2.00	1.00	0.182	6.1	5.9
2.00	1.00	0.462	13.3	13.7
2.00	1.00	0.571	16.2	16.4
2.00	1.00	0.750	21.2	20.4

* The equilibrium constant, K_{12}, used to calculate the EMF values was **2.24×10^{-4} M**.

Table (5-XI)

Conductivities of solutions at high concentrations of organic compounds

Compound R	c(R) Mx10	$c(I_2)$ $Mx10^3$	Conductivity $(\Omega \cdot cm)^{-1} x10^4$	(ratio)	$[I^-]$ $Mx10^3$	(ratio)
Ph_3As	5.00	1.00	0.30		0.12	
				0.13		0.12
TEAI	5.00		2.4		1.00	
Ph_3P	1.00	1.00	1.2		0.38	
				0.50		0.38
TEAI	1.00		2.4		1.00	

5.2-2 Iodine Complexes of Triphenylamine

At high concentrations of organic molecules, the behavior of the triphenylamine-iodine complex was also found to be quite different from the triphenylphosphine and triphenylarsine-iodine complexes.

On addition of I_2 into a colorless triphenylamine solution in 1,2-dichloroethane, the solution turns red-brown and I_3^- is produced, as evidence by the presence of I_3^- absorption band in the UV-visible spectrum. However, as the concentration ratio of Ph_3N and I_2 increased, as shown in Figure (5.6), the absorption by I_3^- increased, instead of decreasing as in the case of Ph_3P and Ph_3As. Intensive I_3^- absorption bands were observed for the solution with concentration ratios of Ph_3N to I_2 up to 1000. Consequently, we can exclude the possibility of reaction (5-18) being one of the equilibrium reaction to form I_3^-. Reaction (5-17), which was found to be the ionization reaction for the Py-I_2 complex, may occur for the Ph_3N-I_2 complexes at high concentration ratios of Ph_3N to I_2.

The fact that reaction (5-18) does not occur for Ph_3N qualitatively shows that Ph_3N forms the weakest bonds with I_2 among the triphenyl group VA compounds.

Moreover, we found that the dissociation mechanism for the triphenylamine-iodine complex is not the same as that for the pyridine-iodine complex in which reaction (5-17) is the only ionization reaction of the complex. The treatment used for the Py-I_2 system[6] does not fit the EMF data for the iodine complex of Ph_3N. Presumably, reaction (5-12), which occurs at high concentration ratios of I_2/Ph_3N, also occurs at low concentration ratios. Quantitative results were not obtained from the EMF data of Ph_3N-I_2 complex at high concentration ratios of Ph_3N to I_2.

It was noted that, when concentration ratios of Ph_3N to I_2 increased to 10:1 or higher, the solution turned green. This was not observed for the other organic compounds. Moreover, when we added TEAI to the green solution, it turned back to an orange brown color. A change was also observed in the UV-visible spectrum, Figure (5.7). It seems possible that the green color has some relation to the complex ion, R_2I^+. Further investigation is necessary to obtain further information about the iodine complex of triphenylamine at high concentrations of Ph_3N.

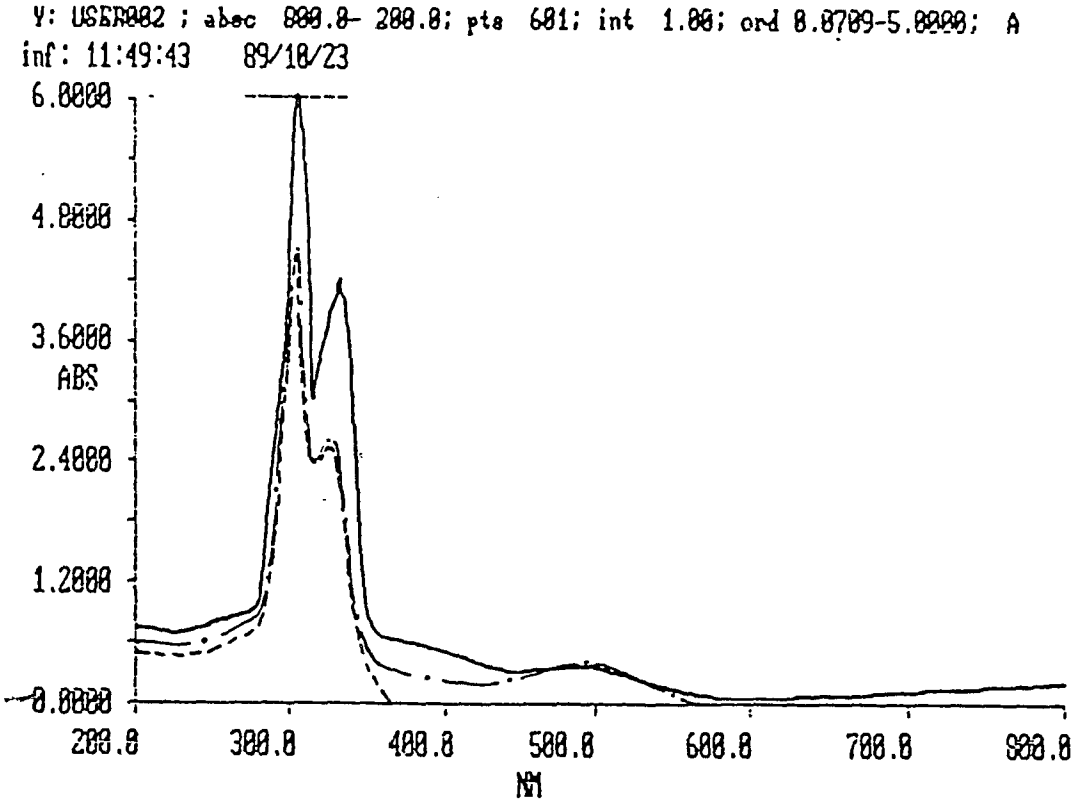

Figure (5.6) : UV-visible spectra of $Ph_3N + I_2$:
——— : $4x10^{-3}$ M Ph_3N, $4x10^{-4}$ M I_2 ;
—·— : $4x10^{-4}$ M Ph_3N, $4x10^{-4}$ M I_2 ;
----- : $4x10^{-4}$ M Ph_3N.

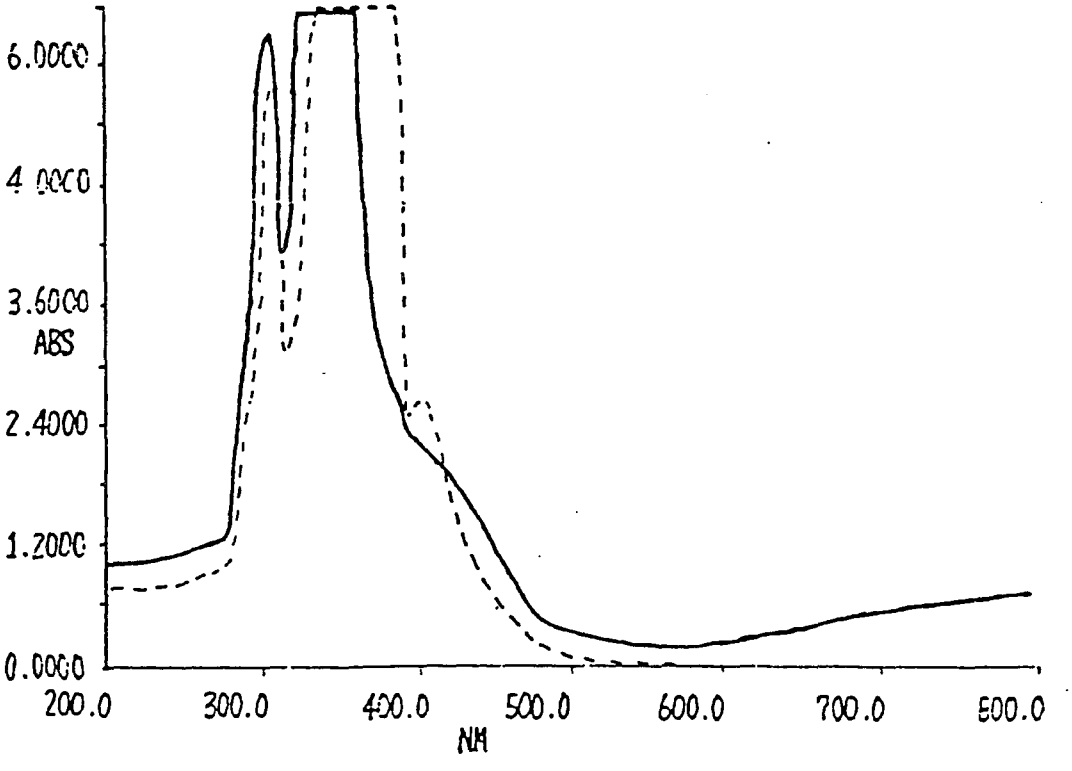

Figure (5.7) : UV-visible spectra of Ph_3N-I_2 system:
——— : $4x10^{-2}M$ Ph_3N, $4x10^{-4}$ M I_2 ;
------ : $4x10^{-2}M$ Ph_3N, $4x10^{-4}$ M I_2 , $4x10^{-4}M$ TEAI.

Chapter 6. ^{31}P NMR MEASUREMENTS OF Ph_3P-I_2 COMPLEXES

The interaction of iodine with triphenylphosphine in 1,2-dichloroethane was studied using ^{31}P NMR. Although a theoretical treatment of the behavior of phosphorus compounds on the basis of chemical shifts is quite complex[32], chemical shifts can be helpful in identifying particular phosphorus compounds.

Since the sensitivity at a given field strength of the ^{31}P nucleus is only 6.63% of that of an equimolar amount of hydrogen because of the smaller magnetic moment[33], we prepared the NMR samples to be as concentrated as possible. However, the concentration of the samples is limited by the solubility of iodine in 1,2-dichloroethane.

^{31}P NMR spectra were measured for solutions with different mole ratios of iodine to triphenylphosphine in order to determine the ^{31}P chemical shifts of the different forms of the iodine complexes.

The spectra obtained in this study appear as a series of sharp signals showing the effects of chemical shifts. The signal narrowing was achieved by broadband proton decoupling and the gain in signal-to-noise ratio was obtained, as needed, by spectral accumulation using Fourier transform techniques. The chemical shift data are all in the form of parts per million from 85% aqueous phosphoric acid, which is the external reference standard.

Triphenylphosphine in 1,2-dichloroethane was identified by a high-field signal at -4 ± 1 ppm, as shown in Figure (6.1). According to Grim and McFarlane's empirical equations[34], the chemical shift of triphenylphosphine is calculated to be -8 ppm.

The intensity of the Ph_3P peak decreased when a small amount of iodine was added into the triphenylphosphine solution. In addition, a

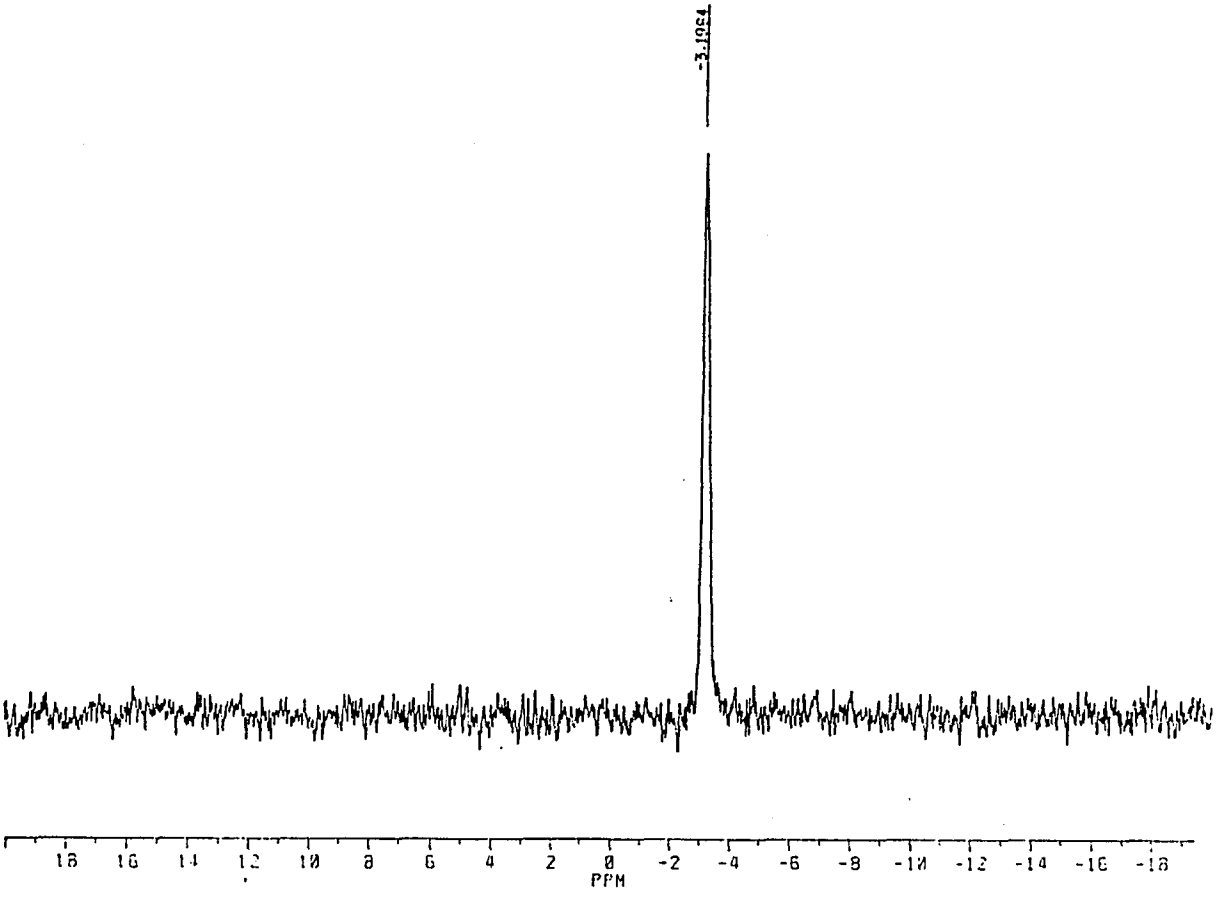

Figure(6.1): ^{31}P NMR spectrum (101.2 MHZ) of Ph_3P in 1,2-DCE

resonance signal at low-field strength was observed. For example, as shown in Figure (6.2), at an I_2 to Ph_3P ratio of 1 to 5, a signal at 38 ppm occurred in addition to the signal at -4 ppm. We assume that the signal at 38 ppm is due to the formation of an iodine complex. As the iodine concentration increased, the signal was found to shift toward lower field strengths, eventually attaining a constant value of 57 ppm.

At a concentration ratio of I_2 to Ph_3P close to 1, the negative chemical shift attributed to Ph_3P disappeared. In addition to the signal at a low-field strength of 38-57 ppm, a new resonance signal at 13 $\pm$ 2 ppm appeared (Figure (6.3)). As the iodine concentration increased, this ^{31}P NMR signal became stronger, whereas the signal at 38-57 ppm became weaker, as shown in spectra (a) and (b) of Figure (6.3).

On the basis of the reaction mechanisms proposed in section 5, reactions (5-1) and (5-2), the above ^{31}P NMR spectroscopic results can be interpreted by assuming that the low-field signal at 38-57 ppm is due to the iodine complex and the signal at 13 ppm results from the formation of the iodine complex cation, Ph_3PI^+.

This interpretation is also supported by the results of the following ^{31}P NMR measurements. 0.05M TEAI was added to a solution with 0.05M Ph_3P and 0.25M I_2. According to reaction (5-2), the concentration of Ph_3PI^+ should decrease and the concentration of Ph_3PI_2 should increase. The ^{31}P NMR spectra in Figure (6.4) show a decrease in the signal at 55 ppm and an increase in the signal at 13 ppm.

Since no ionic complexes are formed in nonpolar solvents, we should see only the unionized complex when iodine and Ph_3P are dissolved in carbon tetrachloride. Our ^{31}P NMR measurements on carbon tetrachloride

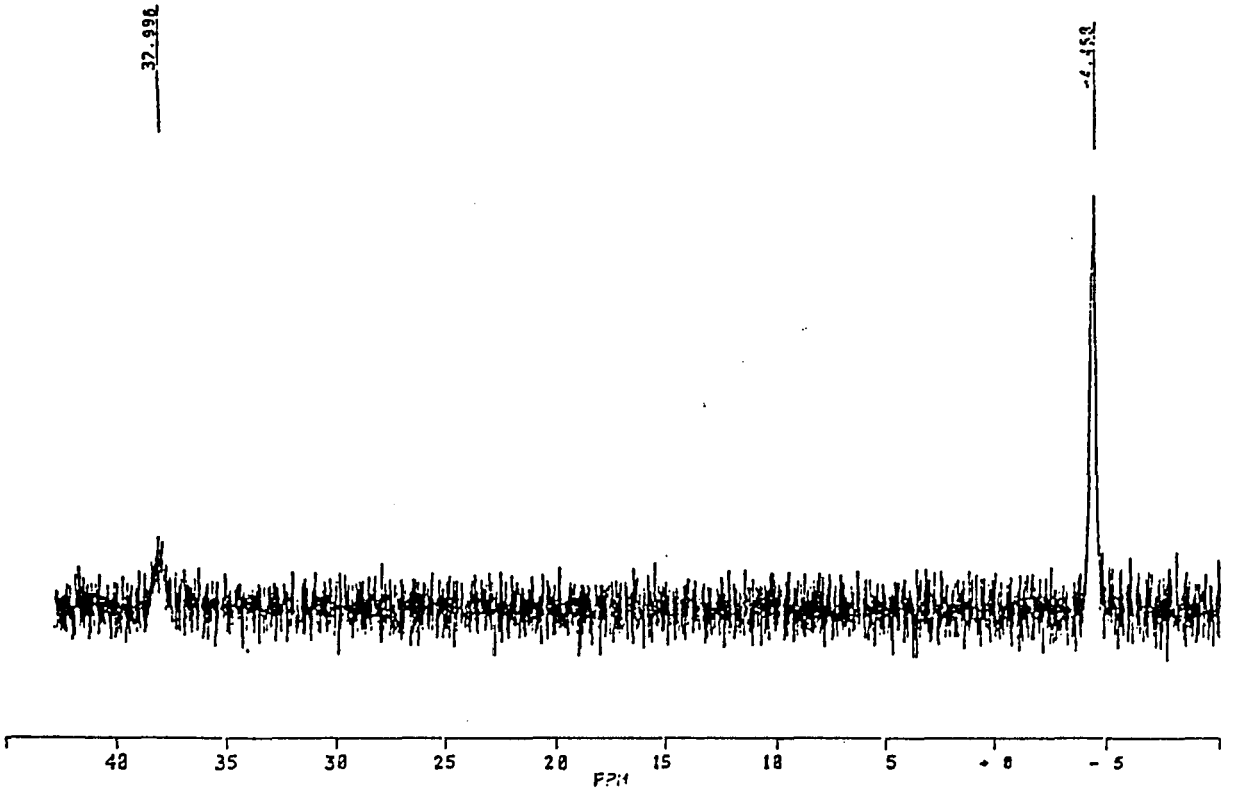

Figure (6.2): ^{31}P NMR spectrum of 0.05M Ph_3P and 0.01M I_2 in 1,2-DCE

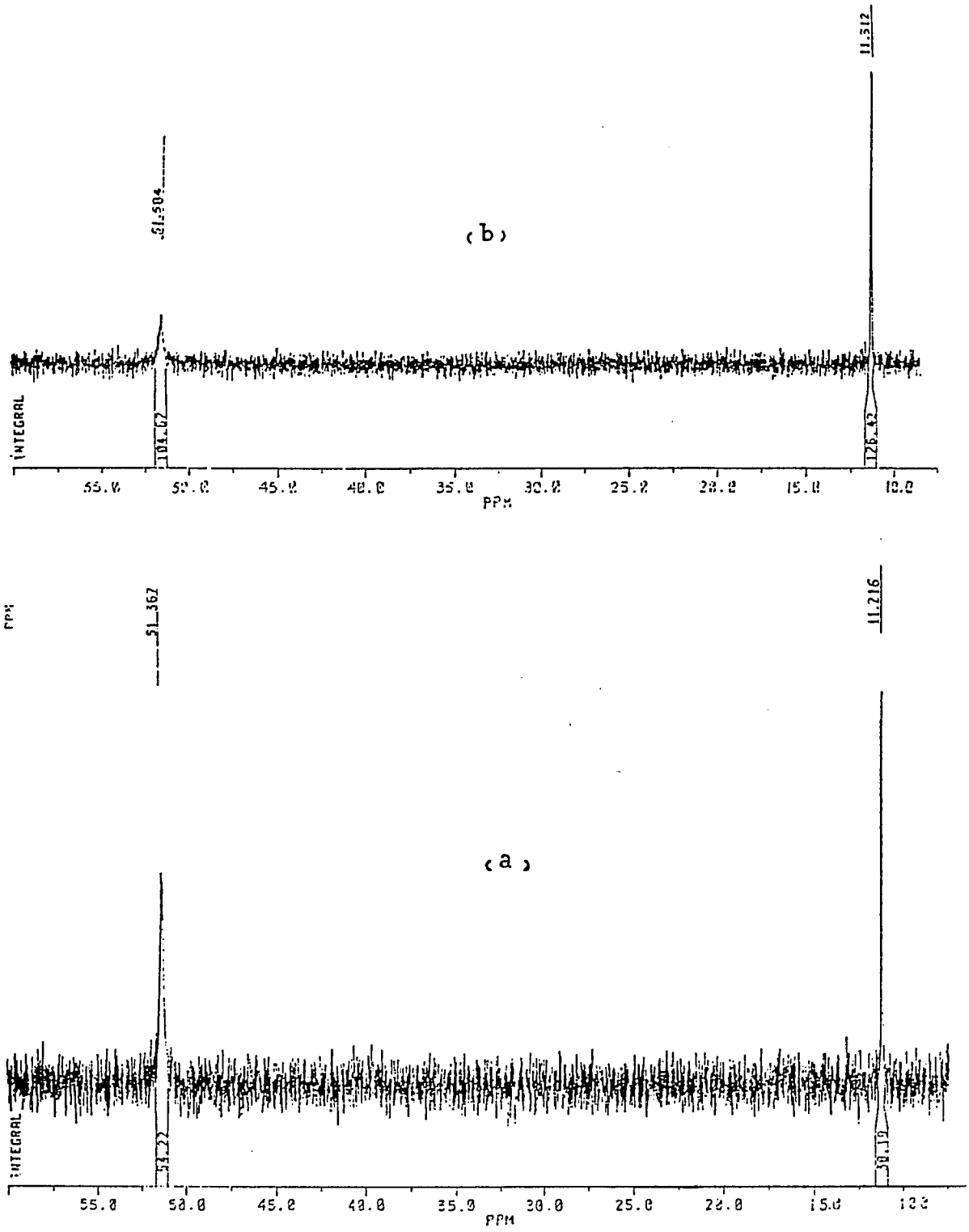

Figure (6.3) : ^{31}P NMR spectra of (a).0.05M Ph_3P, 0.08M I_2 ; and (b). 0.05M Ph_3P, 0.10M I_2 in 1,2-DCE.

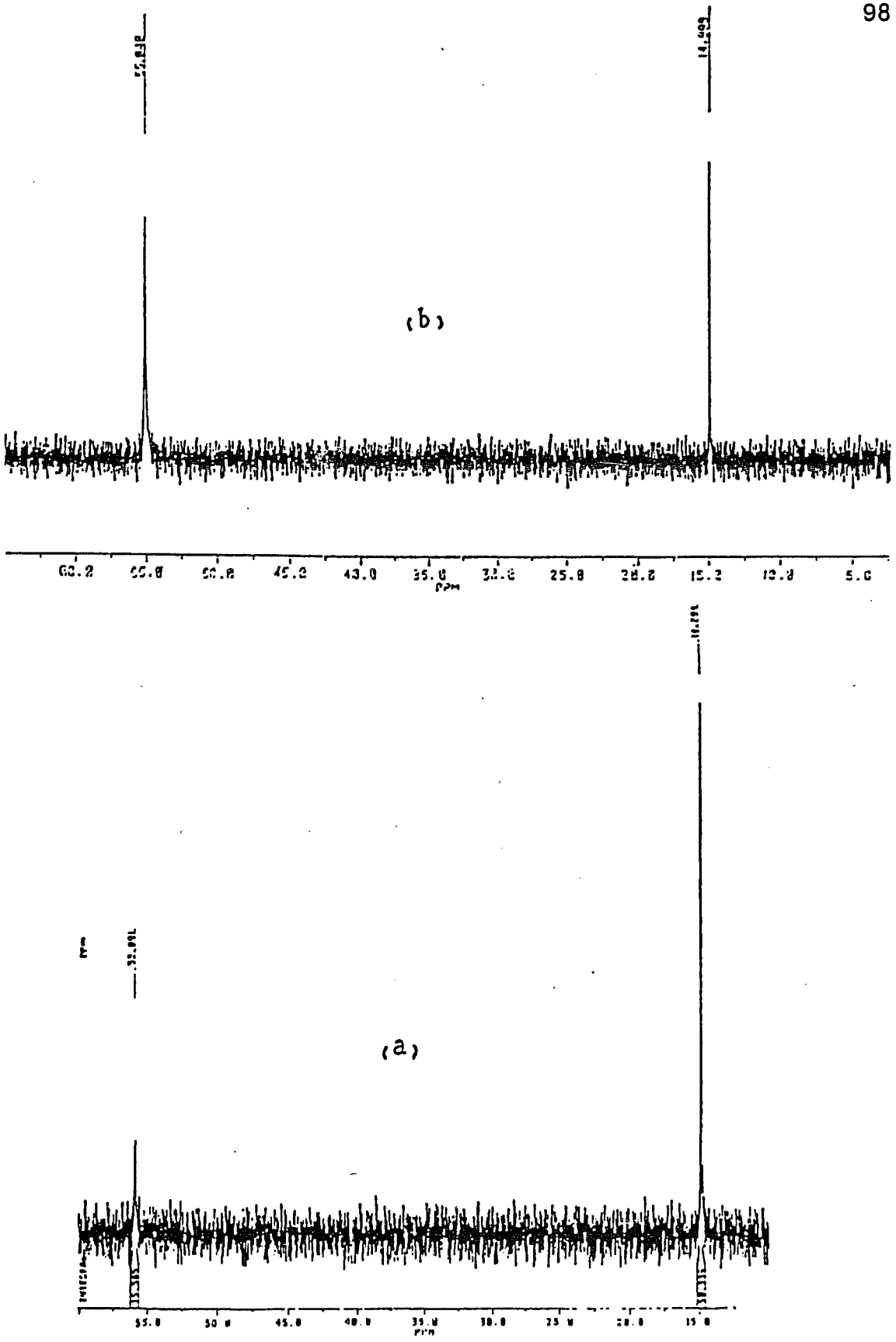

Figure (6.4): ^{31}P NMR spectra of (a): 0.05M Ph_3P, 0.25M I_2 ; and (b): 0.05M Ph_3P, 0.25M I_2 and 0.05M TEAI in 1,2-DCE.

solutions of iodine and triphenylphosphine showed that only a low-field shift of 45 ± 5 ppm occurred (Figure (6.5)), thus reinforcing the validity of our assumption that the shift to this region is due to the unionized iodine complex.

A variation of a few ppm in the chemical shift on the same compound is quite common in a ^{31}P NMR measurement, due to the precision of the measurements with an external reference standard[35]. However, the shift in signal from 38 ppm to 57 ppm as the concentration ratio of iodine to Ph_3P was increased is too large to attribute to experimental variation on a single compound, in this case, Ph_3P-I_2. We suggest that possibly that a chemical exchange mechanism is involved.

The chemical shift values are plotted against the concentration of iodine in Figure (6.6). As we mentioned above, when I_2 is added to the Ph_3P solution, the signal at 38 ppm is shifted to lower field strengths to a limit of about 57 ppm. A possible explanation of this is that the initial signal at 38 ppm arises from the iodine complex, $(Ph_3P)_2I_2$, which occurs at high Ph_3P to I_2 concentration ratios, and the shift at 57 ppm is for the complex, Ph_3PI_2, which occurs at low Ph_3P to I_2 concentration ratios. The exchange reactions which apply are $Ph_3PI_2 + Ph_3P = (Ph_3P)_2I_2$ and $(Ph_3P)_2I_2 + I_2 = 2\ Ph_3PI_2$.

According to the reaction mechanism summarized in reactions (5.1), (5.2) and (5.3), $Ph_3PI_2^{2+}$ should be produced at high iodine concentrations. A signal for $Ph_3PI_2^{2+}$ has not been observed. The probable reason for this is that the concentration of $Ph_3PI_2^{2+}$ is not high enough to produce a measurable resonance signal, the highest concentration of $Ph_3PI_2^{2+}$ produced experimentally was calculated to be 0.002M which is probably not observable by ^{31}P NMR.

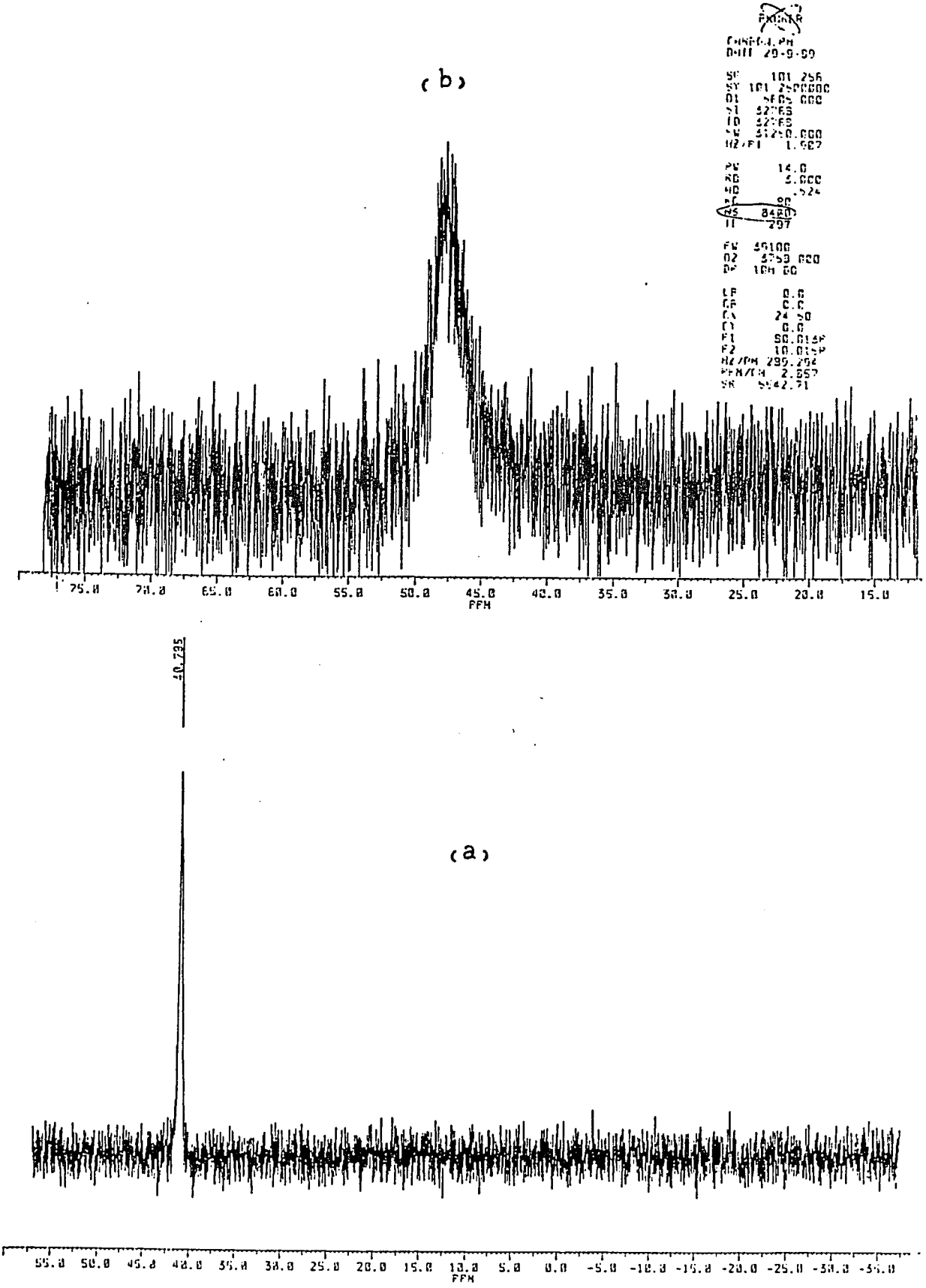

Figure (6.5): ^{31}P NMR spectra of (a):0.04M Ph_3P, 0.02M I_2 and (b): 0.004M Ph_3P, 0.2M I_2 in $\underline{CCl_4}$.

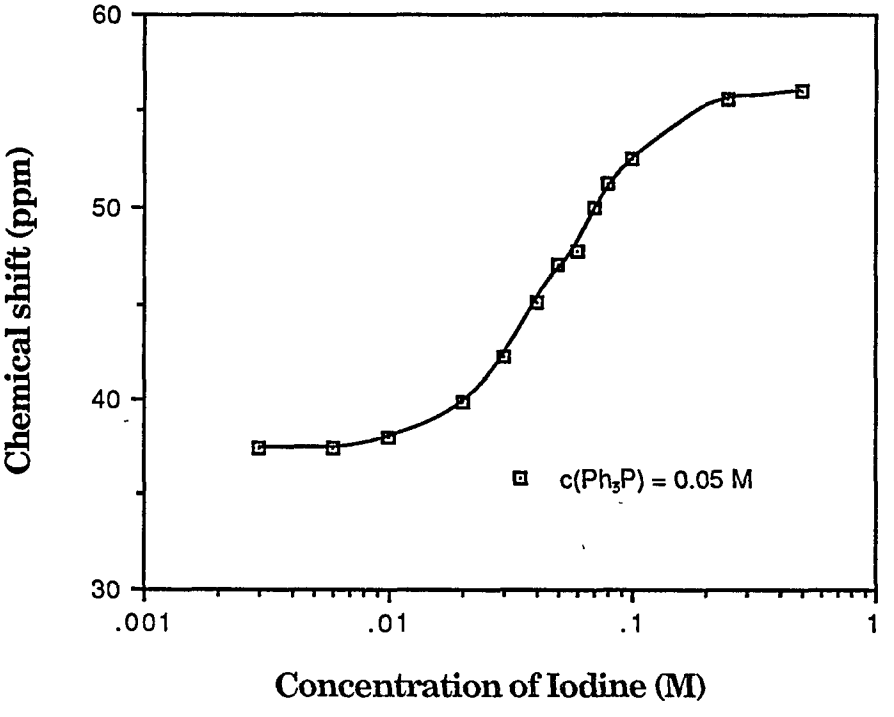

Figure(6.6): Variation of chemical shift with iodine concentration

Appendix A

Mathematical Treatments for the Calculation of Equilibrium Constants at High Iodine Concentrations

The following mathematical treatments were made to obtain values for the equilibrium constants at high iodine concentrations.

A1) High iodine concentrations with equation (5-2) as the only relevant equilibrium reaction:

In this case, the iodine concentration is so high that reaction (5-1) goes completely to the right and equations (5-2) and (5-5) are the primary equations. For side (a) of line-diagram (5-7) (no added TEAI), we have

$$[RI^+] = [I_3^-] = x \; ; \quad [RI_2] = c(R) - x$$

$$[I_2] = c(I_2) - c(R) - x$$

The expression for the equilibrium constant, K_2, in equation (5-5) become

$$K_2 = \frac{x2}{(c(O) - x)\cdot(c(I_2) - c(O) - x)} \qquad (5\text{-}19)$$

For side (b) of line-diagram (5-7) (TEAI added), we have

$$[RI^+] = y \; ; \qquad [I_3^-] = y + c(TEAI)$$

$$[RI_2] = c(R) - y \; ; \qquad [I_2] = c(I_2) - y - c(TEAI) - c(R)$$

The expression for K_2 becomes

$$K_2 = \frac{y(y + c(TEAI))}{(c(O) - y)\cdot(c(I_2) - c(O) - y - c(TEAI))} \qquad (5\text{-}20)$$

The electrochemical equation (5-10) becomes

$$E = -\frac{RT}{F} \ln \frac{x(c(I_2) - y - c(TEAI))^{3/2}}{(y + c(TEAI))\cdot(c(I_2) - c(O) - x)^{3/2}} \qquad (5\text{-}21)$$

Using equations (5-19), (5-20) and (5-21), values for x, y and K_2 can be calculated for each pair of EMF and c(TEAI) values.

A2) High iodine concentrations with equation (5-3) as the relevant equilibrium reaction:

In this case, we assume that reaction (5-2) also proceeds completely to the right. So equations (5-3) and (5-6) are the primary equations.

For side (a) of line-diagram (5-7), we have

$$[RI_2^+] = x\,; \qquad [I_3^-] = c(R) + x$$

$$[RI^+] = c(R) - x\,; \quad [I_2] = c(I_2) - 2c(R) - 2x \approx c(I_2) - 2c(R)$$

The expression for the equilibrium constant, K_3, in equation (5-6) becomes

$$K_3 = \frac{x(c(O) + x)}{(c(O) - x)\cdot(c(I_2) - 2c(O))} \qquad (5\text{-}22)$$

For side (b) of line-diagram (5-7), we have

$$[RI_2^{2+}] = y\,; \qquad [I_3^-] = c(R) + y + c(TEAI)$$

$$[RI^+] = c(R) - y\,; \qquad [I_2] \approx c(I_2) - 2c(R) - c(TEAI)$$

The expression for K_3 becomes

$$K_3 = \frac{y(c(O) + y + c(TEAI))}{(c(O) - y)\cdot(c(I_2) - c(O) - y - c(TEAI))} \qquad (5\text{-}23)$$

The electrochemical equation (5-10) becomes

$$E = -\frac{RT}{F} \ln \frac{(c(O) + x)\cdot(c(I_2) - 2c(O) - c(TEAI))^{3/2}}{(c(O) + y + c(TEAI))\cdot(c(I_2) - c(O))^{3/2}} \qquad (5\text{-}24)$$

Using equations (5-22), (5-23) and (5-24), values for x, y and K_3 can be calculated for each pair of EMF and c(TEAI) values.

Appendix B

Mathematical Treatments for the Calculation of Equilibrium Constants at High Concentrations of Organic Molecules

The following mathematical treatments were made to obtain values for the equilibrium constants at high concentrations of organic molecules.

In this case, equations (5-12) and (5-13) are the primary equations.

For side (a) of line-diagram (5-7), we have

$$[I^-] = [RI^+] = x\ ; \qquad [RI_2] = c(I_2) - x$$

The expression for the equilibrium constant, K_{12}, becomes

$$K_{12} = \frac{x2}{c(I_2) - x} \tag{5-25}$$

For side (b) of line-diagram (5-7) (TEAI added), we have

$$[RI^+] = y\ ; \qquad [I^-] = y + c(TEAI)$$

$$[RI_2] = c(I_2) - y\ ; \qquad [R(a)] \cong [R(b)]$$

The expression for K_{12} becomes

$$K_{12} = \frac{y(y + c(TEAI))}{c(I_2) - y} \tag{5-26}$$

The electrochemical equation (5-16) becomes

$$E = -\frac{RT}{2F} \ln \frac{y}{y + c(TEAI)} \tag{5-27}$$

A value for y is calculated from each experimental EMF value. The equilibrium constant, K_{12}, is, then calculated using equation (5-26).

BIBLIOGRAPHY

[1] Cowan, D. O. ; Wlygul, F. M. ; "The Organic Solid State", Special Report in C&E News, July 21, 1986, 29

[2] Bhat, S. N. ; Rao, C. N. R. ; J. Am. Chem. Soc., **88**, (1966), 3216—3218.

[3] Bao, C. N. R. ; Bhaskar, K. R. ; Bhat, S. N. ; Singh, S.; J. Inorg. Nucl. Chem. **28**, (1966), 1915 to 1925.

[4] Sahai, R. ; Pande, P.C. ; Singh, V. ; Indian. J. Chem. **18A**, (1979), 217 to 220.

[5] Beveridge, A. D. ; Harris, G. S. ; J. Chem. Soc. (1964) 6076.

[6] Aronson, S. ; Wilensky, S. B. ; Yeh, T. I. ; Degraff, D. ; Wieder, G. M. ; Can. J. Chem. **64**, (1986), 2060.

[7] Okamoto, Y. ; Brenner, W. ; "Organic Semiconductors", , Reinhold Publishing Corporpation, New York, (1964).

[8] Berveridge, A. D. ; Harris, G. S. ; Inglis, F. J. Chem. Soc. (A), (1966), 520.

[9] Cotton, F. A. ; Kibala, P. A. ; J. Am. Chem. Soc. **109** (1987), 3308.

[10] Euler, W. E. ; Melton, M. E. ; Hoffman, B. W. ; J. Am. Chem. Soc. **104**, (1982), 5966.

[11] Perissinotti, L. ; Franco, J. I. ; Walsoe de Reca, N. E. ; Solid State Ionics **9/10**, (1983), 453.

[12] Aronson, S. ; Wilensky, S. ; Jawitz, K. ; Teoh, H. ; Polymer **27**, (1986), 101.

[13] Franco, J. I. ; Perissinotti, L. ; Walsoe de Reca, N. E. ; Solid State Ionics **15**, (1985), 101, 95

[14] Mulliken, R. S. ; Person, W. B. ; "Molecular Complexes -- A lecture and reprint volume" J. Wiley, New York. (1969) 266-287, 147, 354-356

[15] Cotton, F. A. ; Wilkinson, G. ; "Advanced Inorganic Chemistry". Wiley, New York. (1980).

[16] Andrew, E. R., Nuclear Magnetic Resonance, Univ. Press: Cambridge, 1955

[17] Gerenstein, D. G., Ed. "Phosphorus-31 NMR Principles and Applications" Academic Press: New York, 1984.

[18] Allerhand, A. ; Gutowsky, H.S. ; Jonas, J.; J. Am. Chem. Soc., **88**, (1966), 3185

[19] Gutowsky, H. S. ; Holm, C. H. ; J. Chem. Phys. **25**, (1956), 1688.

[20] Hannay, N. B.; "Solid-State Chemistry". Prentice-Hall, Inc., Englewood Cliffs, New Jersey. (1967)

[21] Mott, N. F.; "Organic Liquid Semiconductros" Phil, May, 24,1.(1971)

[22] Van der Pauw, L. J. ; Philips Research Reports. **13**, No.1, (1958), 1-9

[23] Van der Pauw, L. J. ; Philips Technical Review. **20**, (1958-1959), 220-224

[24] Aronson, S. ; Liss, A. ; Hirsh, R. ; J. Chem. Phys. **66**, No.2. (1977), 877.

[25] Wagner, C. "Thermodynamics of Alloys" Addison-Wesley Publishing Co., Inc.

[26] Daly, J. J. ; J. Chem. Soc. **10**, (1964), 3799

[27] Soboley, A. N. ; J. Organometal Chem. **179**, (1979), 153-157

[28] Mente, D. C. ; Mills, J. L. ; Inorg. Chem. **14**, (1975), 123

[29] Degraff, D. ; "Thermodynamic Stability and Electrical Conductivity of Halogen Complexes of Organic Solids -- A Ph.D. Disseration". The City Uniersity of New York. (1987)

[30] Nigretto, J. M. ; Jozefowicz, M. ; Electrochim. Acta, **19**, (1974), 809.

[31] Aronson, S. ; Epstein, P. ; Aronson, D. B. ; Wieder, G. ; J. Phys. Chem. **86**, (1982), 1035

[32] Muller, N. ; Lauterbur, P. C. ; Goldenson, J. ; J. Chem. Phys., **78**,(1955), 3557-3561

[33] Jones, R. A. Y. ; Katritzky, A. R. ; Angew. Chem. internat. Edit., **1**, No. 1, (1962), 32-40.

[34] Grim, S. O.; McFarlane, W. Nature, (London), **208**, (1965), 995.

[35] Verkade, J. G. ; Quin, L. D. "Methods in Stereochemical Analysis Vol.8 — Phosphorus-31 NMR Spectroscopy in Stereochemical Analysis". VCH Publishers, Inc., Deerfield Beach, Florida. (1987), 96, 89